RESEARCH TRIANGLE INSTITUTE

RTI/1825/01-01 F

NASA CR 165675

FEASIBILITY OF COLLISION WARNING, PRECISION APPROACH AND LANDING USING THE GPS

FINAL REPORT

VOLUME ONE

Prepared For

NASA

National Aeronautics and Space Administration
Langley Research Center
Hampton, Virginia

RESEARCH TRIANGLE PARK, NORTH CAROLINA 27709

FEASIBILITY OF COLLISION WARNING, PRECISION APPROACH AND LANDING USING THE GPS

Final Report

Prepared Under Contract NAS1-15833

By

W. H. Ruedger

Research Triangle Institute
Research Triangle Park, North Carolina 27709

Prepared for

NASA

National Aeronautics and Space Administration
Langley Research Center
Hampton, Virginia

March 1981

PREFACE

This report was prepared by the Research Triangle Institute, Research Triangle Park, North Carolina, under Contract NAS1-15833. The work has been administered by the Avionics Technology Research Branch of the Flight Electronics Division, Langley Research Center, National Aeronautics and Space Administration. Mr. W. E. Howell served as Technical Representative.

Program studies began on 23 May 1979 and were completed on 22 July 1980. Mr. R. D. Alberts served as Laboratory Supervisor and Mr. W. H. Ruedger as Project Leader. Dr. N. G. Staffa assembled the data pertaining to the ionospheric considerations, Dr. D. R. Daluge performed the ranging simulation and Mr. J. V. Aanstoos provided the data link structure definition, the collision avoidance system functional description and compiled the CAS survey contained as Appendix F.

TABLE OF CONTENTS

LIST OF FIGURES

LIST OF TABLES

LIST OF TABLES continued

1.0 INTRODUCTION

The Research Triangle Institute (RTI) has, under contracts NAS1-14302 and NAS1-14719, investigated various aspects of the potential avionics capability which may become available to general aviation by exploitation of the Global Positioning System (GPS). GPS is a satellite-based navigation system being developed by the Department of Defense and having accuracies on the order of ten meters in position and one-twentieth of a knot in velocity, both in three dimensions. GPS also has the capability for providing the user a very precise time estimate.

As a part of the effort completed under the more recent contract (NAS1-14719), RTI has defined conceptual approaches wherein GPS may be used, with an appropriately configured data link, to enhance general aviation avionic functions encountered in the terminal area and on approach. During the current study, RTI has further examined the extent of this enhanced capability. Functions specific to this study are approach and landing guidance and collision warning.

One effort of this study explored the feasibility of using differential GPS to obtain the precision navigation solutions required for landing. The study established that the concept is sound and developed an experimental program with the objective of demonstrating this concept. Other effort, of comparable emphasis, generated the foundation and guidelines involved in the use of GPS, with an associated data link, to provide collision avoidance and/or warning. This effort examined the collision avoidance/warning concept through the development of a functional system specification. The development of an experimental program to demonstrate the validity of the concept will likely be the subject of a still-to-be-defined future study.

2.0 STUDY OBJECTIVE

The objective of this study was to evaluate the feasibility and resultant potential for general aviation of operation of GPS in a differential mode. The feasibility of differential mode operation is approached through an examination of ionospheric effects by a literature search and through simulation. The potential for general aviation is explored through an examination of the terminal area capabilities afforded by the precision of differential operation.

3.0 DIFFERENTIAL GPS CONCEPT

3.1 Introduction

This section provides a discussion of considerations involved in the feasibility demonstration of GPS in a differential mode, as applied to the landing problem, and of considerations in configuring the associated data link to use the GPS for collision avoidance and/or warning.

During a previous study [3-1], several promising concepts were developed using navaids in conjunction with a data link. The observation that the major error source in the GPS error budget is due to the ionospheric delay correction process, and observing that for Omega, ionospheric uncertainities are compensated by operation in a differential mode, leads to the concept of differential GPS. The elements of GPS in a differential mode are shown in Figure 2-1. The focal point of the system is the monitor station, which typically would be located near the runway, and which consists of a high performance GPS receiver and a data link to local users. Since the monitor station may be very accurately surveyed into position, any deviation in position from the survey as observed by the monitor-located GPS receiver is an indication of offset due to system or propagation error (at the monitor). With the assumption that these offsets are both temporally and spatially correlated, as will be discussed further in the following paragraphs, they can be used by other dynamic users to correct their position fixes. The offset information can be provided in the form of pseudorange corrections, code position corrections, four-dimensional position corrections, etc. The mechanism for providing this data to the user implies the specification of a broadcast type data link.

Spatial correlation is required in that the observed ionospheric group delays at the monitor and at the user locations need to be nearly the same. This requires that the total electron count in the "monitor transversal" and in the "user transversal," as shown in Figure 2-1, be equivalent. Preliminary review [3-2] of the literature indicates that spatial variation of the ionosphere is on the order of hundreds of kilometers, which is the right order-of-magnitude for the application. Also note that if the monitor is at the runway threshold, spatial variation effects tend to zero as touchdown is neared. This then alludes to the feature available with differential GPS, which is the use of stand-alone GPS en route with graceful transition to differential mode for increasing precision during approach and landing.

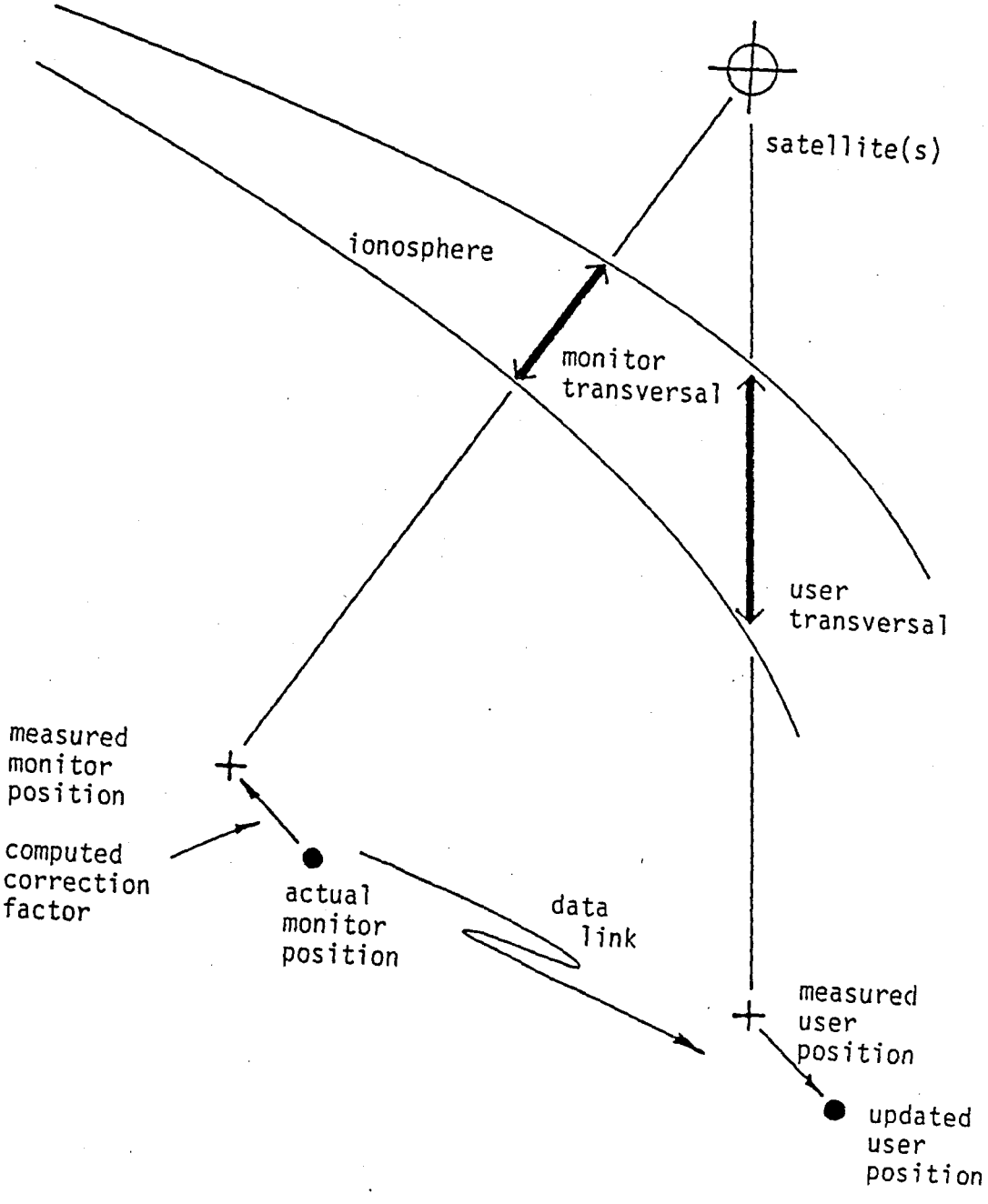

Figure 2-1. Differential GPS geometry

Consideration of the degree of temporal correlation is required in that the monitor must first measure and then relay these offsets to the user. This results in a finite time delay before the data may be applied in a corrective manner. This means that ionospheric turbulence must be stable over periods comparable to the delay time and the navigation update rate. Again, the literature tends to support this [3-3], although much of the electron density sounding data available represents averages taken over relatively long (on the order of minutes to hours) time windows.

Provided these considerations are in accord, the concept of differential GPS provides a way to reduce, and possibly eliminate, the error associated with the ionospheric delay correction and, in doing so, may provide a measure of relative code position (i.e., code offset is the correction factor elected). This then gives rise to a mechanization which can hopefully provide two-channel, P-code performance with a single-channel, low-cost configuration. A major task under this study is the development of an experimental program to demonstrate this performance.

3.2 Differential GPS Considerations

The following paragraphs discuss various considerations associated with the differential GPS concept and reflect aspects which influence conceptual design as well as performance evaluation. The list is not exhaustive but merely representative. Table 2-1 lists the topics to be covered.

Performance Improvement - As mentioned previously, the major contribution of error in the GPS pseudo-range computation is that of the ionosphere group delay calculation. Table 2-2 shows a compiled error budget as given in [3-4]. Assuming these errors to be uncorrelated and taking the RSS, one obtains an RMS error of 4.04 meters. Further assuming that differential mode can drive the ionospheric error to zero and repeating the calculation, a RMS error of 2.7 meters is obtained. Carrying the calculation still further and postulating that all bias and Markov errors can be compensated for in the differential mode, an RMS error of 1.43 meters can be calculated. It should be remarked that this line of argument is not intended to validate accuracies on the order of a meter but rather to provide the stimulus (in the form of potential performance) for a demonstration and evaluation of the achievable performance in differential mode.

Table 2-1: Differential GPS Considerations

Performance Improvement

User Convenience

Reliability

Size of User Community and Compatibility with a High-Density Collision Avoidance System

Monitor Correction Broadcast Rate

Overspecified Constellation Broadcast (as Aid in Constellation Update)

Optimal Constellation Prediction-Based on Monitor Measurement of Ionospheric Conditions

Monitor Fault Detection and Alarm

Use of Tracking Antennas for Monitor

Monitors Linked to Provide Ionsopheric Survey

Performance vs. Range from Monitor

Combination of Differential and Standalone Inputs

Monitor Provision of Code Offset as Acquisition Aid

Monitor Assist During Dropouts and in Multipath

Monitor Location

Handover Concept

Table 2-2 GPS NAVIGATION ERROR SUMMARY [3-4]

Error Contributor	Pseudorange	Statistics	Notes
Satellite Ephemeris	1.5 meter	Bias	Uncorrelated between Satellites
Satellite Group and Clock	1.0 meter	Bias	Uncorrelated between Satellites
Pseudorange Noise	1.0 meter	Markov	Evaluated at C/N_0 = 30 db for P-Code
Range Quantization	0.226 meter	White Noise	
Range Mechanization Error	1.0 meter	White Noise	
Ionospheric Dual Frequency	3.0 meter	Markov	Evaluated at C/N_0 = 30 db for P-Code. No Averaging
Tropospheric Residual	1.0 meter	Bias	Evaluated at 5° evaluation and zero altitude
Multipath Error	1.0 meter	White Noise	

User Convenience - For the user to effectively utilize the equipment, it is important that the transition from normal GPS navigation to differential navigation be transparent to him. It is important, however, that he know in a very positive manner under which mode he is currently operating. It is further important that the user be alerted in case of transition from differential to normal mode so that he can be aware of the reduced accuracy during critical segments of his flight profile.

Reliability - As voiced in previous studies, the reliability/graceful degradation afforded by a multichannel receiver reconfigurable to a lower performance profile in the case of failure is a distinct GPS advantage over other approaches. The extension of this to GPS in a differential mode simply involves considering the impact of the reconfiguration of the monitor receiver on the accuracy of the ionospheric correction update.

Size of the User Community and Compatibility with a High Density Collision Avoidance System - Since the differential concept involves deployment in the terminal area, user community size is significant only for the handful of heavily congested air terminals. It should be added that differential mode likely has its highest cost/benefit for the smaller, more poorly instrumented air fields where high traffic density is not a problem. The need for landing support and collision avoidance still is a requirement for these terminals as well.

Monitor Correction Broadcast Rate - With a four-channel receiver, the monitor can presumably transmit ten correction updates a second. This is much faster than either of the requirements of landing or collision avoidance. A bound on how slowly the correction can be updated can be obtained from the four-second update on current surveillance radar instrumentation. Note that the traffic density does not impact the update rate in that the aircraft do not have to be individually addressed for update transmission.

Constellation Broadcast - As an aid in acquisition, it is possible to broadcast the current optimal constellation set. This would reduce user equipment complexity (i.e., he would not have to evaluate the geometry) at the expense of negating stand-alone operation. The optimal set of satellites could be predicted based on both current ionospheric conditions as well as GDOP factors.

Monitor Fault Detection and Alarm - An important feature of the monitor receiver is fault detection and subsequent alarm broadcast. Consideration should be given the measure of signal quality and the calculation of monitor error for broadcast in addition to an all-out fault. Provision for some degree of fault-tolerance would be easily accommodated by a four-channel reconfigurable approach

Use of Tracking Antennas for Monitor - To achieve a high signal level so as to minimize monitor induced error, tracking or rotating antennas would be beneficial. This would significantly increase monitor cost possibly at the expense of optimal constellation prediction.

Monitors Linked to Provide Ionosphere Survey - As an aside to the main theme of the study, it should be mentioned that, as is pointed out in a subsequent section, global data defining the behavior of the ionosphere at L-Band is virtually non-existent. The network of differential GPS monitor stations, properly instrumented would provide an excellent laboratory for recording the behavior of the ionosphere both spatially and temporally.

Performance Versus Range from Monitor - The accuracy with which the monitor can update a user equipment output is a function of user distance from the monitor site. This develops into a paradox in where to site the monitor. Best accuracy likely would result in a landing situation with the monitor at the threshold. However, this results in maximum dynamic range requirements on the user equipment. As the monitor is moved away from the runway, both the geometry and ionosphere spatial de-correlation affect performance. It will be recommended in later sections that the monitor be mounted in a van and this consideration be the theme of an experiment.

Combination of Differential and Standalone Modes - In certain situations the differential mode can introduce errors which may degrade performance over that achievable with standalone mode. A way to monitor this to avoid degradation is to compare the correction offset with the error budget of the user equipment and to flag the condition when the correction exceeds some fraction of the specific user equipment error. This requires the user to communicate his receiver configuration to the monitor and some degree of additional processing to occur at the monitor. This now impacts the limitation on total capacity in that the monitor is now required to address each user aircraft uniquely. A simplistic approach would be the use of a maximum range from the monitor for which differential mode is valid. Since the user knows the co-ordinates of the monitor he is using, this computation could occur autonomously in the user aircraft.

Monitor Provision of Code Offset as Acquisition Aid - It is likely that since the monitor continuously tracks the code, it could broadcast a predicted code offset based on estimated user position as a code acquisition aid.

Monitor Assist During Dropouts and Multipath - Although nothing of particular innovation surfaced during the course of this study, the availability of the monitor station should not be overlooked in providing support during user dropouts and in multipath conditions.

Handover Concept - The correction handover from monitor to user can be considered in two categories. The first would apply correction within the receiver mechanization and would require hardware modification. Examples include carrier phase offset, code delay offset, or pseudo-range error. These are probably the most accurate but also have significant hardware impact. The second is to apply correction by using local position offset and performing the correction with software after uncorrected user position has been estimated by the receiver in the aircraft. This is less accurate but its simplicity of implementation makes it an excellent candidate for an experimental program.

4.0 IONOSPHERIC CONSIDERATIONS

4.1 Introduction

This section presents those considerations in establishing the feasibility of GPS in a differential mode from the point of view of the variability of the ionospheric propagation group delay. As has been stated elsewhere, the position error must be well correlated spatially and temporally in the satellite-user-monitor geometry. The following discussion attempts to establish this correlation by characterizing the ionosphere at L-band through the conduct of a review of relevant literature and then the utilization of these data as the parameters in a ranging simulation which produces spatial and temporal error over an ensemble of conditions.

The literature review produced the following nominal parameters as representative of ionospheric conditions:

Spatial Gradient: 10^{15} E/M^2 per 100 KM
Maximum Disturbance Density: 10^{17} E/M^2
TID* Propagation Velocity
1200 M/SEC MAX
100-150 M/SEC Nominal

From this it can be concluded that the ionosphere can be characterized by slow moving electron densities on the order of 10^{15} E/M^2 or less.

Utilizing these data in the ranging simulation, the following observations were made:

1. Range error is fairly insensitive to geometry (i.e., a factor of two over the cases examined)
2. The range error is linear with electron density
3. The best results occur at 90° elevation which is in concert with good vertical accuracies.
4. Nominal electron densities produce residual range error of less than one meter.

These observations support the conclusion that ionospheric effects do not preclude operation in a differential mode. The following paragraphs discuss these points in more detail.

*Traveling Ionospheric Distribution

4.2 GPS Ranging Errors as a Function of User Distance from Monitor Station and Time from Correction Update

A user of the GPS will find his position by computing his distance from several satellites. Distances are computed by measuring differences in time from when the signal was sent to when received and multiplying by c, the speed of light. However, the signal speed changes slightly as the signal passes through the ionosphere and the troposphere. This creates a time delay which is interpreted as an increase in distance or path length of the signal. Thus, there is an error in computed position. This error could be corrected by using information sent to the user from the nearest monitor station. The monitor station, knowing its own true location, also computes its location from the satellite signals in the same manner as the user. The difference between computed and known positions is sent to the user to be used as a correction to his computed position. The accuracy of this correction depends on how nearly equal are the signal delays experienced by the monitor station and the user. Spatial variations in the ionosphere or troposphere cause the correction to be in error for the user since user and monitor are "looking" through different sections of the atmosphere. One would expect this error to increase with the distance from the monitor station. Likewise, if the characteristics of the atmosphere were changing in time, the error in the correction would also be increasing with the time from its last computation.

The difference in the signal delays experienced by the user and monitor station can be expressed as a distance by multiplying by the speed of light. This is an implied satellite ranging error. The increase of this error with distance from the monitor station will be expressed as a gradient in millimeters per kilometer. Likewise, the increase with time from last computation will be expressed as a rate in millimeters per second.

These atmospheric effects on the use of GPS are similar to problems experienced by aperture synthesis radio telescope systems. In both cases, the extraterrestrial radio sources are being "viewed" from different positions on the earth's surface through different sections of ionosphere and troposphere. A major difference is that telescopists are concerned with phase velocity and phase differences while GPS is affected by changes in signal velocity and signal delay. However, telescope experience is very valuable since phase velocity and signal velocity are simply related.

A very useful paper by Hinder and Ryle [4-1] describes all atmospheric sources of error affecting long baseline radio telescopy. This treatment has served as a guide for evaluating all possible phenomena affecting the use of GPS. Other applicable literature was also searched to verify or modify their conclusions as they apply to GPS. Rare incidents which would cause large errors in use of GPS were also sought. Time variation in the atmospheric effects as applied to GPS were also deduced from the body of literature studied.

Tropospheric Effects

In the troposphere, phase velocity is independent of wavelength. Since this implies no dispersion, a group velocity and path length equal to that reported for phase is assumed. Differences in path length of an extra-terrestrial signal passing through the troposhere to two receivers some horizontal distance apart are due to three effects:

Small Scale Irregularities - These vary in size from 300 to 1200 meters and may cause differences in path length up to 6 mm on a summer day. The effect is usually smaller, expecially at night or in winter. Thus, an intrinsic error of 6 mm is set for any stations separated by more than 300 meters.

Large Scale Weather Systems - These are associated with gradients of pressure and humidity which could cause path length errors as much as 20 mm/100 km for certain orientations. Hinder and Ryle surmise that even larger gradients may at times exist. They also surmise that ground-based measurements could be used to correct such errors to within 20%. Since the initial estimate, .2 mm/km, is much smaller than possible ionospheric effects, it seems unnecessary to correct for them. Furthermore, it could be expected that the maximum gradient exists only at the front, and the total error over a long baseline is less than the product of the gradient times the baseline.

Curvature - This effect occurs because two separated receivers do not acquire a source at the same elevation angle. Thus, path length through the troposphere is different. The difference in path length through the troposphere increases drastically at low elevation angles. This is seen in Table 4-1 taken from Hinder and Ryle.

Table 4.1: Differential Path in mm Due to the Curvature of the Atmosphere for a Source at an Azimuth Along the Baseline.

Baseline (km)	Elevation (In Degrees)			
	5	10	20	45
1	38	11	3	1
10	380	110	28	5
100	3800	1100	280	50

For radio telescopy, Hinder and Ryle estimate that a correction could be made to within 10% of these path differences. This, however, implies a simple tropospheric model and knowledge of the elevation angle of the source.

Ionospheric Effects

Range Error and Electron Content - At frequencies above 1 GHz, the index of refraction for radio waves in the ionosphere is everywhere real and less than 1. Thus, the phase velocity is greater than c. The group velocity, however, is less than the speed of light. It can be shown, however, that in the range of frequencies and electron densities of interest, the group velocity is smaller than c by the amount that the phase velocity exceeds c (Appendix A).

The difference in path length experienced by the signal or phase in traversing the ionosphere is proportional to the total electron content in a column along the ray path. For the phase, Hinder and Ryle give:

$$L = -4.5 \times 10^{-16\ 2}\ Q \text{ meter}/(\text{m}^2 \text{ electrons}/\text{m}^2)$$

where L is phase path increase and Q is columnar electron content. This gives

$$L/Q = -16.2 \text{ cm}/10^{16} \text{ electrons}/\text{m}^2$$

for $L_1 = 1.575$ GHz ($\lambda = .190$ m)*

and $L/Q = -26.6 \text{ cm}/10^{16} \text{ electrons}/\text{m}^2$

for $L_2 = 1.2325$ GHz ($\lambda = .243$ m)*

The formula cited by Philco-Ford [4-2] for change of signal path length (R):

$$R = (1.32(Iv/f^2)/10^{16} \text{ electron}/\text{m}^2) \text{ ft } (\text{GHz})^2$$

gives the same absolute lengths where Iv is the total content and f is the frequency. Thus, it is evident that phase difference measurements, when

*L_1 and L_2 are the dual frequencies associated with the GPS.

expressed as length, can be taken over directly to this work with, at most, a scaling by the ratio of the square of wavelengths.

Ionospheric Variations. Variations in total electron content as a function of horizontal position (gradients) or time (rates) may cause the computed position correction to be in error for the user. The range error associated with these rates and gradients can be expressed in millimeters per second from the time of last measurement and millimeters per kilometer horizontal distance from the base station. Sources of these variations are irregularities, diurnal variations, solar flares and geometrical factors.

Irregularities. Hinder and Ryle divide irregularities into small, medium and large scale. The medium and small scale irregularities are responsible for radio star scintillations and spread F. They also include the medium scale traveling ionospheric disturbances (TID). The most extensive study of irregularities of size from 10 km to over 400 km was done by J. E. Titheridge [4-3]. The most interesting result of this study was that the change of total integrated vertical electron content with horizontal distance was not a function of the size of the irregularity. Hinder and Ryle, citing Titheridge and other investigators claim these gradients are between .5 and 2 x 10^{15} electrons/m^2 per 100 km. This would give a maximum range error of 53 mm/100 km at 1.23GHz. Examining Titheridge's paper shows that this gradient is the slope of the line fitting the logrithmic plot of electron content vs. size of the irregularity. It could easily be expected that the average gradient be twice that number Moreover, within the first quartile of the size group of irregularities centered on 420 km are electron contents of 1.7 x 10^{16} electrons/m^2. Assuming this change occurs within 200 km gives a gradient of 8.5 x 10^{15} electrons/m^2/100 km or 2.3 mm/km at 1.23GHz. He reports that 92% of the irregularities had electron contents under 10^{16} electrons/m^2, but allows that he has seen changes of 10^{17} electrons/m^2. Since the size of this irregularity is not known, it is uncertain as to what was the maximum gradient seen out of the 2650 irregularities studied, but 10 mm/km might very well be possible. This is confirmed by isolated incidents in some other studies done with arrays of radio telescopes. Warwick, Davis and Spencer [4-6] report a phase difference of 3 radians at 962MHz over 24 km near Jodrell

Bank. This translates into a gradient of 4 mm/km at 1.23GHz. However, J. P. Hamaker [4-7] in his paper reporting measurements of phase gradients over a 1.3 km array displays a graph of phase gradient vs. time for April 7, 1971. Gradients of 13 mm/km at 1.4 GHz are seen. This would translate to 17 mm/km at 1.23GHz. However, he notes that such large gradients have not been seen in studies by Warwick et al. with their 24 km baseline. Although Hamaker is quite unsure of what conclusions to draw, it may be that such large gradients do occasionally exist, but on a scale less than 15 km. Yet, it could be that large scale, large gradient phenomena exist, but only very seldom.

Titheridge's study was limited by the extent of the ionosphere he could observe - about 1,000 km. Larger structures have been observed [4-1] and their velocities measured [4-7, 4-10]. These velocities span a range of 400 to 760 m/sec. These are north to south travelling waves; whereas, the smaller scale sizes are generally characterized as east-west travelling. Little information on these disturbances is available. Garriott et al. [4-4] display a profile of electron content vs. time of day after an ionospheric storm. A decrease of 1.4×10^{17} electrons/m^2 out of 8×10^{17} electrons/m^2 is attributed to a travelling ionospheric disturbance. The gradient associated with this TID can be estimated from the time of passage and a guess at the velocity. Estimating 2 hours from the graph and using the slowest speed measured by Chan and Villard [4-5] (1,450 km/hr = 403 m/sec) gives a gradient of about 5×10^{13} electrons/m^2/km or 1.3 mm/km. Thus, it is quite possible that the largest horizontal gradients are seen in the medium to small scale irregularities and not in the large scale TID.

Summarizing available information on horizontal gradients in electron content due to ionospheric irregularities, it seems that almost all gradients would be less than 10 mm/km at 1.23GHz with the possibility that on very rare occasions, larger gradients may occur. In stating this number as a maximum gradient, it should be noted that most of the time gradients of less than one-half that value would obtain.

When any of these irregularities travel in a horizontal direction, the vertical electron content changes in time. The rate of this change is the product of the horizontal gradient and the velocity. Measurements of velocity have been made by several observers [4-10 through 4-14]

and range up to 1,200 m/sec, but with averages around 100 to 150 m/sec. Unfortunately, no attempt has been made to correlate size and magnitude with speed which might better limit maximum rate. Taking a more likely 800 m/sec velocity and a maximum gradient of 10 mm/km gives an expected maximum rate of 8 mm/sec. Notice must be taken that 5 mm/km x 150 m/sec = 0.75 mm/sec is much more likely to be experienced.

Diurnal Variations. The quantity of ionization is directly due to the action of solar radiation and is a strong function of the solar zenith angle. Thus, horizontal gradients of vertical electron content exist as well as a rate of change as the earth moves under the ionization pattern. Hinder and Ryle report that maximum rates of 10^{13} electrons/m^2/sec occur shortly after dawn. The profile of Garriott et al. [4-4], mentioned previously, shows rates as high as 7.4 x 10^{13} electrons/m^2/sec occurring after an ionospheric storm, while other profiles show rates about 5 x 10^{13}/m^2/sec. Moreover, using Martyn's [4-8] maps of maximum electron density contours and deducing the total vertical content vs. maximum density ratio from vertical electron density profiles [4-15], a rough calculation (Appendix B) yields approximately 1.4 x 10^{14} electrons/m^2/sec at the equator for one area of one of the maps.

Taking all these factors into consideration, a choice of 10^{14} electrons/m^2/sec may be taken as a rare maximum of diurnal gradient in a solar active year, and 5 x 10^{13} electrons/m^2/sec a more typical maximum. Dividing these rates by the tangential speed of the earth at 30° latitude (.4 km/sec) yields gradients of 2.5 x 10^{14} and 1.3 x 10^{13} electrons/m^2/km or 6.7 mm/km and 3.4 mm/km at 1.23GHz. The rate of change in range for these maxima would be 2.7 mm/sec and 1.4 mm/sec. Thus is seen, as in the case of ionospheric irregularities, a degree of uncertainty. The rates and gradients produced by each effect are, to the degree that they are known, approximately of the same magnitude.

Solar Flares. A source of sudden change in columnar electron content is solar flares. Garriott, da Rosa, Davis and Villard [4-16] have documented five events in which the total electron content changes about 2 x 10^{16} electrons/m^2 in two minutes. The total change was about

5%. At 1.23 GHz this corresponds to a rate of change in range of 4mm/sec. This rate does not continue for more than two minutes, however.

Geometric Effects. As with the troposphere, because of the curvature of the earth two separated observers look through different thicknesses of ionosphere at the same source. Hinder and Ryle report the magnitude of this effect as a function of elevation angle for a source in the direction of the line between observers. Reproduced here from their data is the differential path computed for wavelength = 24 cm. Also given are values for intense ionization conditions.

Table 4-2. Differential Path vs. Elevation (λ = 24 cm)

	Elevation			
	5°	10°	20°	45°
typical	1.2 mm/km	1.7 mm/km	1.4 mm/km	.5 mm/km
maximum	12 mm/km	17 mm/km	14 mm/km	5 mm/km

This effect, of course, has a cosine dependence on the azimuthal angle of the source from the connecting baseline and a variation with azimuth due to whatever diurnal or latitude gradient that may be present.

The other variations in total vertical columnar electron content mentioned previously must all be multiplied by a geometric factor due to the increase in path length through the ionosphere with increase in zenith angle. Appendix C gives a table of this increase computed from a simple slab model. Because of the height and curvature of the ionosphere, this factor is at most 3 and is less than 2 for zenith angles less than about 65° or elevation angles greater than 25°.

Summary

Tropospheric effects are negligible when compared to ionospheric effects, except when the source is viewed at low elevation angles along the line separating the viewers. Gradients of 40 mm/km are then possible. This translates to a signal delay difference of 0.13 nanoseconds per kilometer of horizontal separation. This effect could be accounted for to 10% of this value by employing a simple model.

Absolute maximum gradients and rates due to the ionosphere are given in Table 4-3 for 1.23GHz as deduced from the sources mentioned. Delay differences in nanoseconds (ns) are also given.

Table 4-3. Ionosphere Variability from Various Sources

Type	Gradient		Rate	
Irregularity	10 mm/km	.03 ns/km	8 mm/sec	.026 ns/sec
Diurnal	7 mm/km	.02 ns/km	3 mm/sec	.01 ns/sec
Flare			4 mm/sec	.013 ns/sec
Curvature	17 mm/km	.06 ns/km	(10° elevation, azimuth along baseline)	

The geometric effects (curvature) could be accounted for to within 20% by a simple model, if necessary. It is also believed that these numbers reflect conditions which occur only rarely. If more information were available and the appropriate correlations made between occurrence, time of day, solar cycle, etc., a good statistical study would probably show gradients and rates of one-half to one-fifth these values to be usual.

Spatial Correlation

In an attempt to address the notion of spatial correlation, the following comments were exerted from a work by Klabuchar and Johanson [4-19] relating to correlation distance of mean daytime content.

Correlations in total electron content (TEC) were calculated for pairs of stations having separations of from 1,500 to 5,000 km as shown in Figure 4-1. This was done both for stations oriented east and west (longitudinal separation) and stations oriented north and south (latitudinal separation). Simple linear relationships between separation and average correlation are

$$R = 1 - .0001d/\text{kilometer}$$

where R is the linear correlation coefficient and d is the separation. For north-south the relation is

$$R = 1 - .000165d/\text{kilometer}.$$

These correlations predict improvement in prediction over using monthly means. The percent reduction in uncertainty is given by

$$P = \%\ \text{improvement} = 100\ [1-(1-R^2)^{\frac{1}{2}}].$$

The percent of improvement, the correlation necessary and the distances over which that correlation obtains are given in Table 4-4. As a check on the results, data was gathered from graphs of monthly correlations for four pairs of sites.

Error bars also appeared on the graph so that weighted least squares linear fits of the data could be made. When this was done for east-west data using only the data supplied, the intercept at zero distance was $.942 \pm .01$ and the slope was $(-.669 \pm .04) \times 10^{-4}$/km. This is in agreement with the slope of the line in their figures and indicates that the distances calculated in Table 4-4 might be slightly pessimistic.

To make use of these results to predict possible absolute error, one needs to know the absolute uncertainty associated with prediction of TEC by using monthly means.

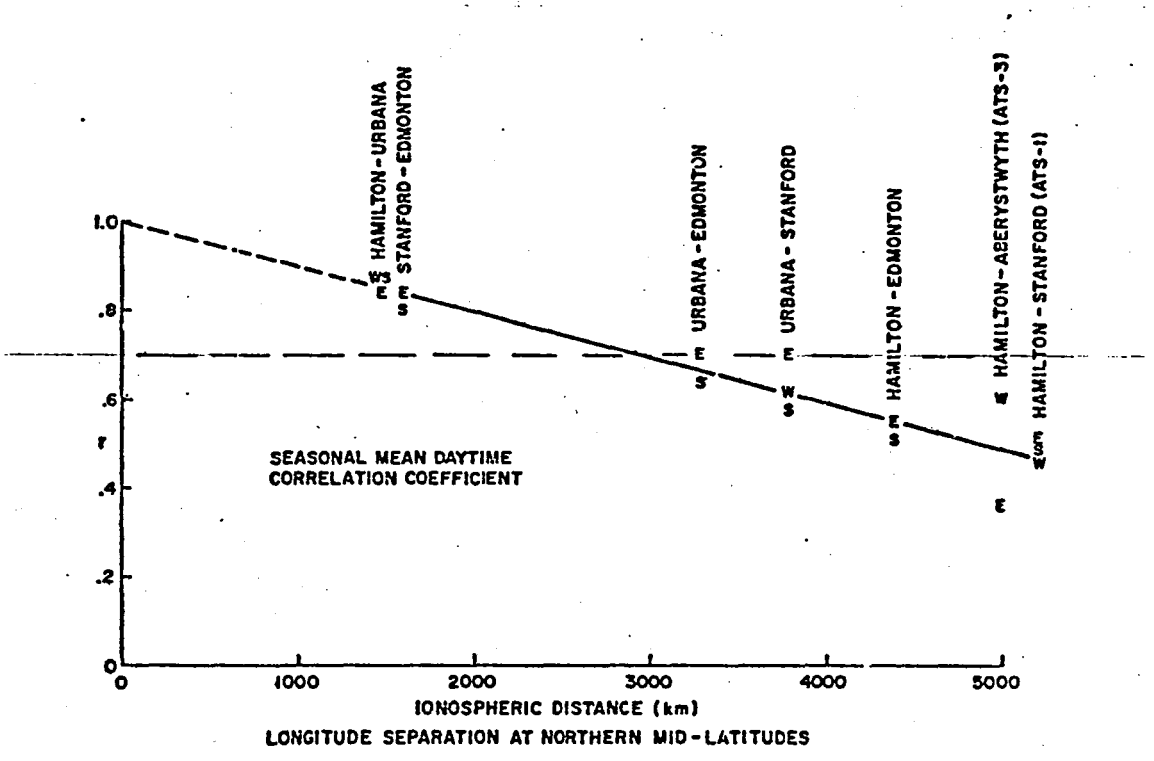

Figure 4-1. Linear relation of correlation vs. east-west distance [4-19].

Table 4-4. Extrapolation of [4-19] to Small Separations and High Values of Correlations

fractional predictive improvement	necessary linear correlation coefficient	E-W separation kilometers	N-S separation kilometers
0.2500000	0.6614378	3385.622	2051.892
0.3000000	0.7141429	2858.572	1732.468
0.3500000	0.7599342	2400.658	1454.944
0.4000000	0.8000000	2000.000	1212.121
0.4500000	0.8351647	1648.353	999.0020
0.5000001	0.8660254	1339.746	811.9670
0.5500001	0.8930286	1069.714	648.3114
0.6000001	0.9165152	834.8483	505.9686
0.6500001	0.9367498	632.5024	383.3348
0.7000001	0.9539393	460.6074	279.1560
0.7500001	0.9682459	317.5414	192.4493
0.8000001	0.9797959	202.0407	122.4489
0.8500001	0.9886860	113.1397	68.56954
0.9000002	0.9949874	50.12572	30.37922
0.9500002	0.9987492	12.50803	7.580627
1.000000	1.000000	0.0000000	0.0000000

4.3 Differential GPS Ranging Simulation

Overview

A GPS user and a nearby monitor station receive the satellite ranging signal. The monitor, knowing its true range from the satellite, can provide the user with a good estimate of ionospheric delay, with which the user estimates his range. He will be in error because 1) his calculation occurs slightly later than that of the monitor station and 2) his position is slightly different from that of the monitor.

In the simulation, spatial and temporal ionospheric variations are simulated by introducing an anomaly into a baseline ionosphere comprising several spherical shells of uniform electron density. Refraction at the shell surface interfaces and delay within the shells are simulated using vector ray-trace methods. The satellite-user path contains the anomaly, while the satellite-monitor path does not. This is shown geometrically in figure 4-2.

In the ionosphere, the speed of light is calculated from

$$\left(\frac{C}{V_p}\right)^2 = 1 - \frac{Ne^2}{\pi\nu^2 m}$$

and

$$V_p \cdot V_g = C^2$$

where

V_p = phase speed of light (used in refraction calculation)

V_g = group speed of light (used in delay calculation)

C = speed of light in vacuum

N = electron concentration

e = electron charge

ν = signal frequency

m = electron mass

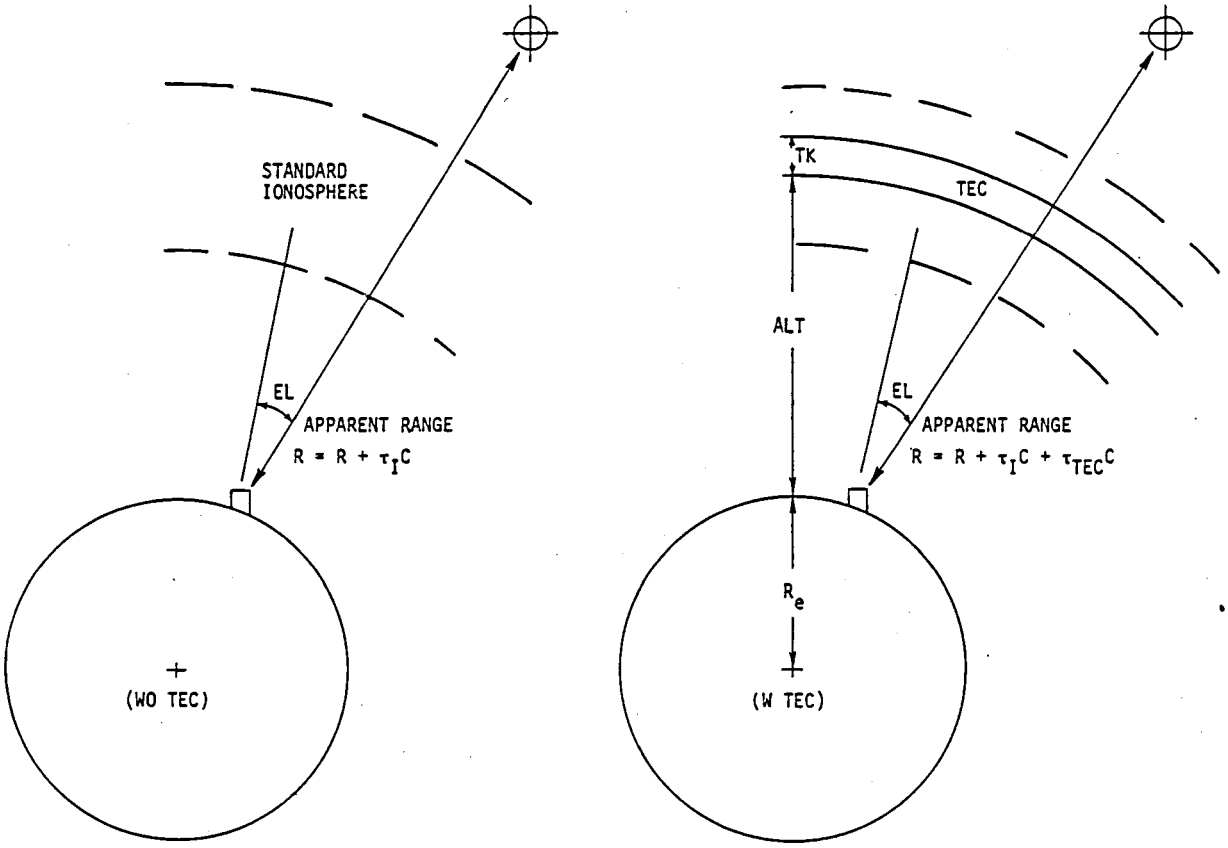

Range Error

$$\Delta R = \tau_{TEC} C = R^{1} - R$$

Standard Ionosphere

15 Shells

$N_e = 1.86 \times 10^{18} e/m^2$

Daytime Maximum During Sunspots

Simulation Parameters

Disturbance Altitude
Disturbance Thickness
TEC
Elevation Angle
Surface Offset (Between W and WO Disturbance)

Figure 4-2. Simulation geometry.

Note that

$$\frac{C - V_g}{C} = \frac{C - \frac{C^2}{V_p}}{C} = 1 - \frac{C}{V_p} = 1 - \sqrt{1 - \frac{Ne^2}{\pi \nu^2 m}}$$

is the error in range per unit path length caused by using the speed of light in vacuum instead of the true group speed in the delay calculation (for straight-line paths). This expression may be approximated by a Taylor's series:

$$\frac{C - V_g}{C} = .5X + .375X^2 + .3125X^3 + .2734375X^4$$

where $X = \frac{Ne^2}{\pi \nu^2 m}$

Note that $X < 10^{-4}$, even for the very large concentrations which occur during the day at the peak of the sunspot cycle.

Intersection of a Vector with a Spherical Shell

A vector of the form

$$\vec{R}_o + \rho\vec{U}$$

where $\vec{U}$ is a unit vector intersects a spherical shell of radius R_s, centered at the origin at a distance ρ, which may be determined by solving

$$\left(\vec{R}_o + \rho\vec{U}\right) \bullet \left(\vec{R}_o + \rho\vec{U}\right) = R_s^2$$

The solution is the smaller root of

$$A\rho^2 + B\rho + C = 0$$

where

$$A = \vec{U} \cdot \vec{U}$$

$$B = 2\vec{U} \cdot \vec{R}_o$$

$$C = \vec{R}_o \cdot \vec{R}_o - R_s^2$$

On a digital computer, best accuracy is obtained by solving for ρ as

$$\rho = \frac{2C}{-B + \sqrt{B^2 - 4AC}}$$

A Vector Description of Refraction

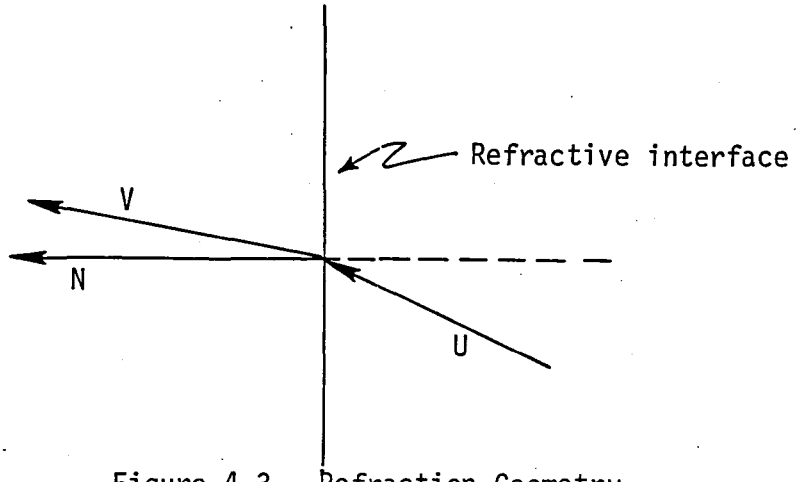

Figure 4-3, Refraction Geometry

In figure 4-3, $\vec{U}$ is the unit incidence vector and $\vec{V}$ is the unit refracted vector. The vector $\vec{N}$ is the unit normal on the side opposite $\vec{U}$.

The vector equation of refraction is

$$\frac{C}{V_{pi}}\left(\vec{U} \times \vec{N}\right) = \frac{C}{V_{pr}}\left(\vec{V} \times \vec{N}\right)$$

where V is a unit vector of the form

$$\vec{V} = a\vec{U} + b\vec{N}$$

These conditions imply that

$$a = \frac{V_{pr}}{V_{pi}}$$

and that

$$b = \frac{V_{pr}}{V_{pi}}\left\{\sqrt{\left(\frac{V_{pi}}{V_{pr}}\right)^2 + \left(\vec{U}\cdot\vec{N}\right)^2 - 1} - \vec{U}\cdot\vec{N}\right\}$$

(When the critical angle is exceeded, the root in the expression for b is undefined and the ray undergoes total internal reflection.)

The Ionospheric Model

The Earth is modelled as spherical in the ranging simulation and the ionosphere is modelled as consisting of several concentric shells of distinct, uniform electron densities.

These densities were chosen to simulate daytime during a sunspot maximum (see Figure 4-4).

Specifically, the altitudes and electron densities were:

ALTITUDE (km)	DENSITY (e/cm^3)
60 - 100	400
100 - 160	220000
160 - 240	500000
240 - 320	3000000
320 - 400	2700000
400 - 500	2100000
500 - 600	1700000
600 - 700	1500000
700 - 800	1400000
800 - 900	1200000
900 - 1000	1150000
1000 - 1500	190000
1500 - 2000	100000

The effect of satellite elevation on ionospheric delay depends upon the specific patterns of altitudes and densities. For near 90° elevation, the effect of the multi-layer ionosphere is essentially the same as that of a single layer with the same total electron content.

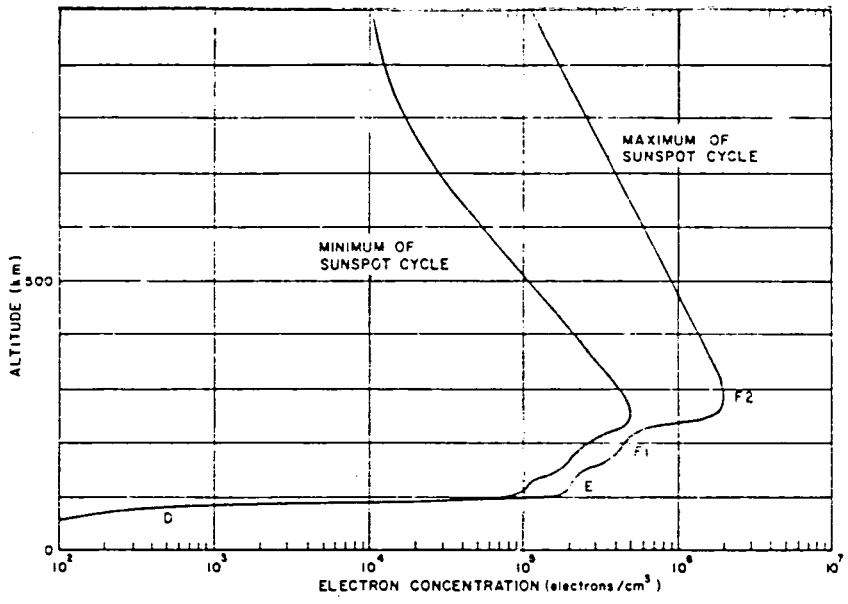

a. Daytime.

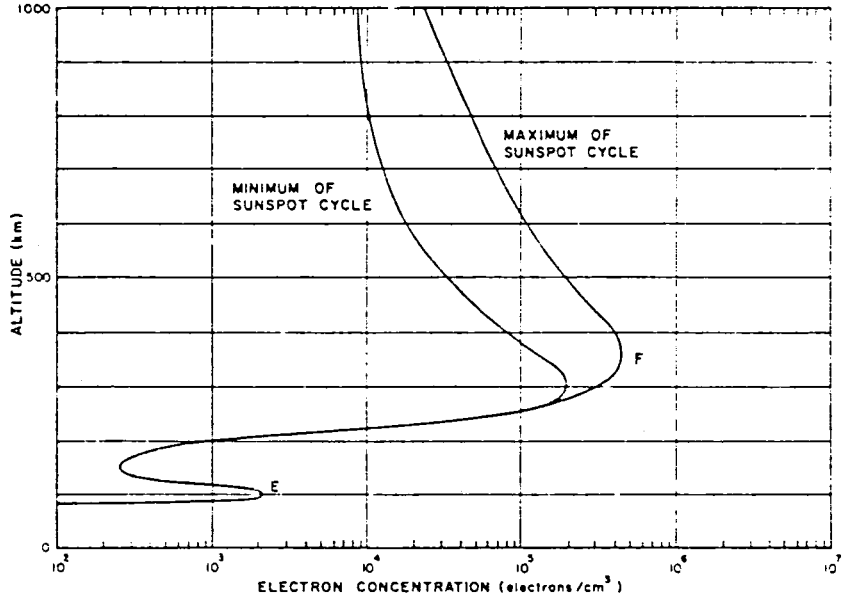

b. Nighttime.

Figure 4-4. Normal electron distributions at the extremes of the sunspot cycle [4-15].

4.4 Simulation Results

The simulation was run for the set of parameters shown in Table 4-5. A summary of the results is given in the following figures. Tabular results are contained in Appendix D.

Table 4-5. Differential GPS Parameter Set

ALTITUDE	100 - 300 - 900 km
THICKNESS	100 - 300 - 900 km
TEC	10^{15} - 10^{16} - 10^{17} e/m^2
OFFSET	0 - 10 - 100 km
ELEVATION	5 - 10 - 30 - 90 degrees

Simulation Program

A flow chart of the simulation program is shown in figure 4-5. A program listing is included as Appendix E.

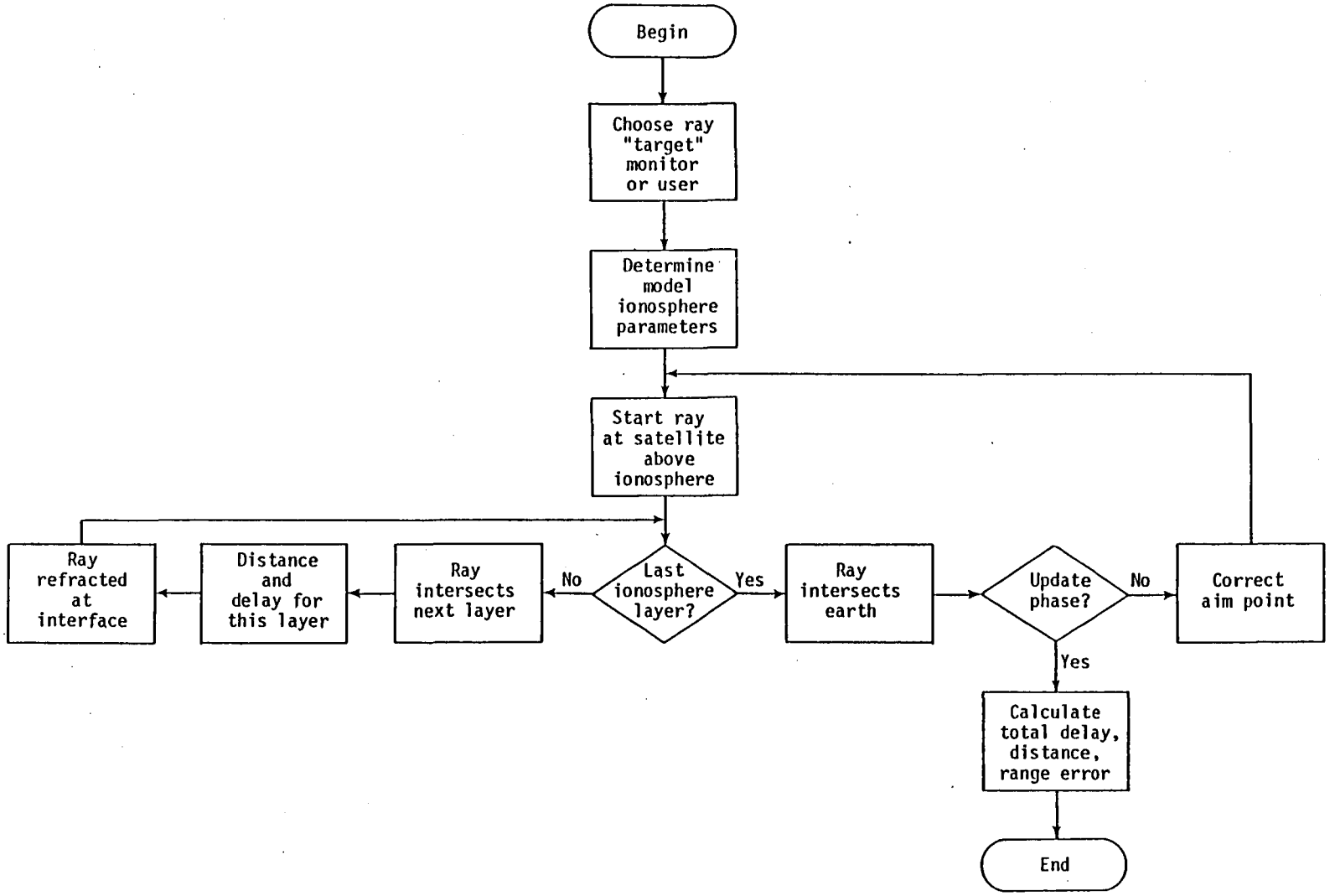

Figure 4-5. Differential GPS ranging simulation flowchart.

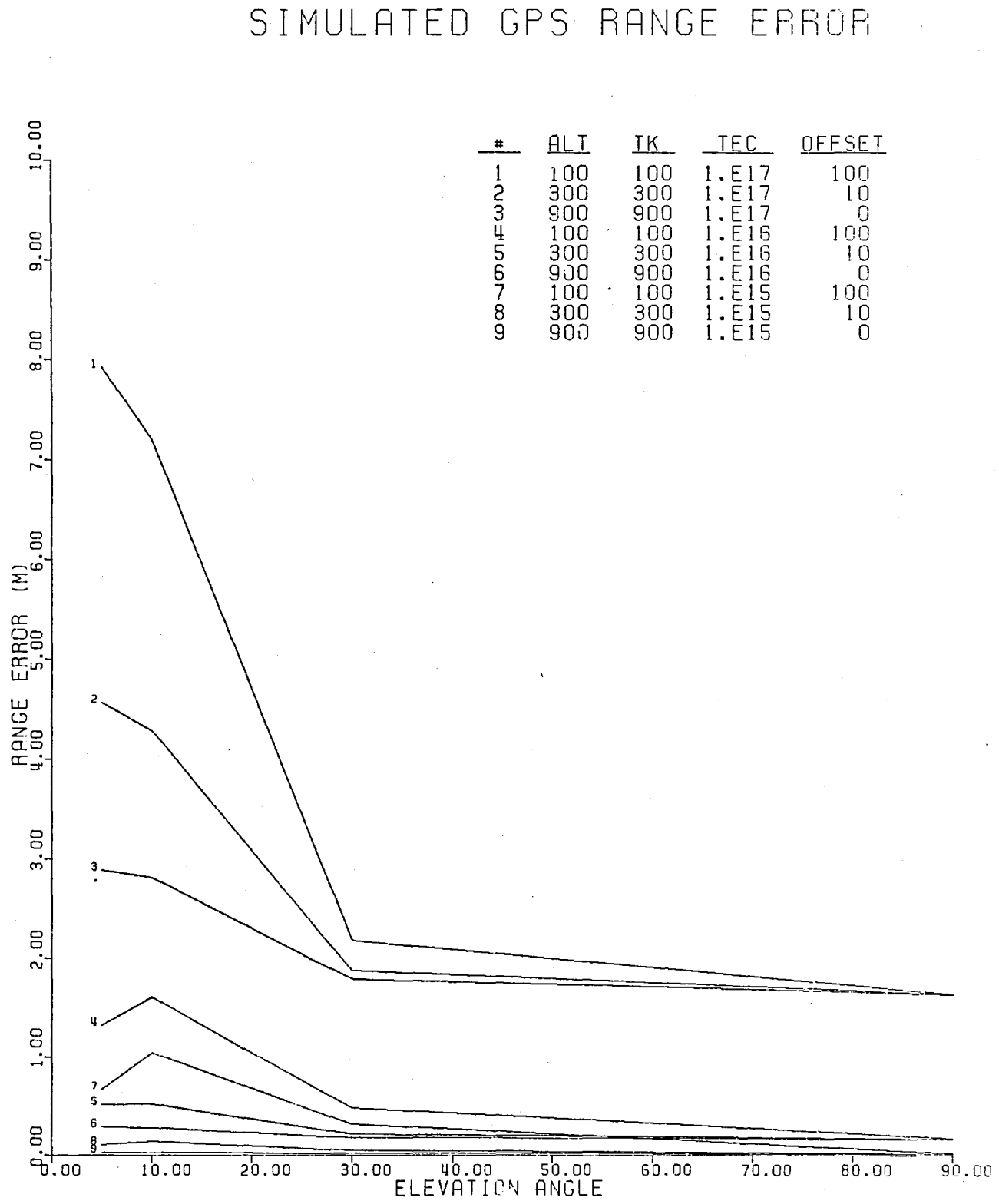

Figure 4-6. Simulation summary.

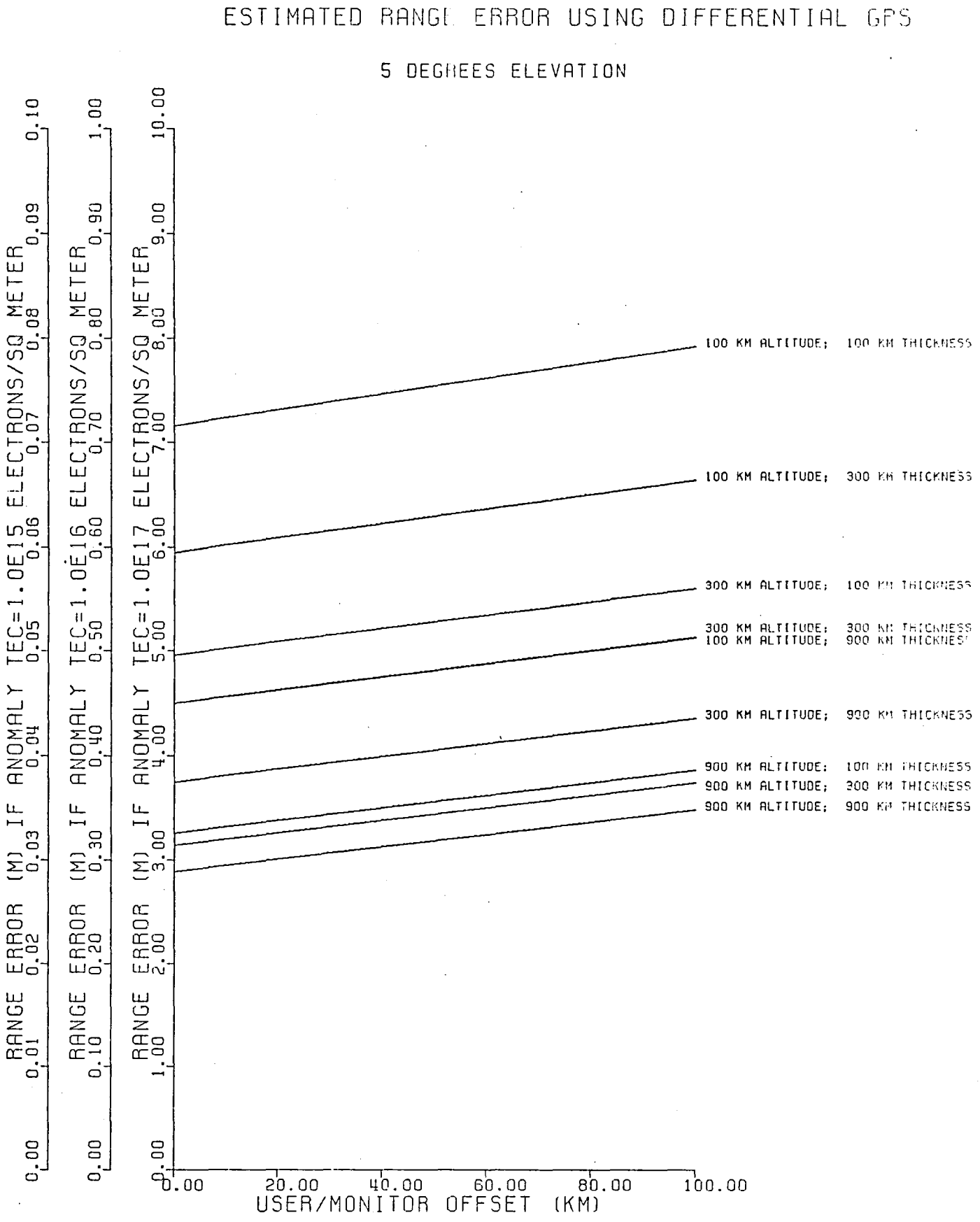

Figure 4-7. Range error at 5^{0} elevation.

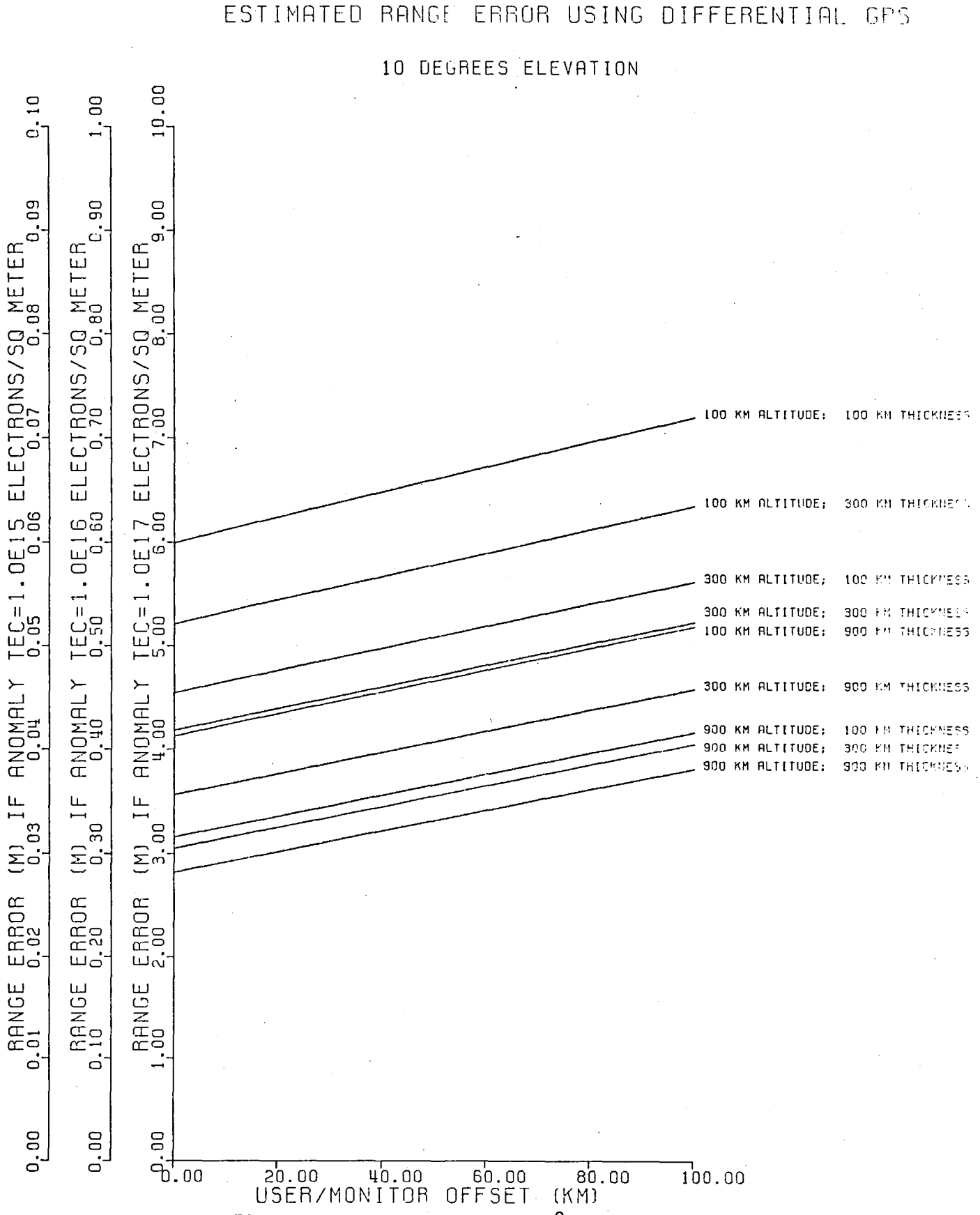

Figure 4-8. Range error at 10^{o} elevation.

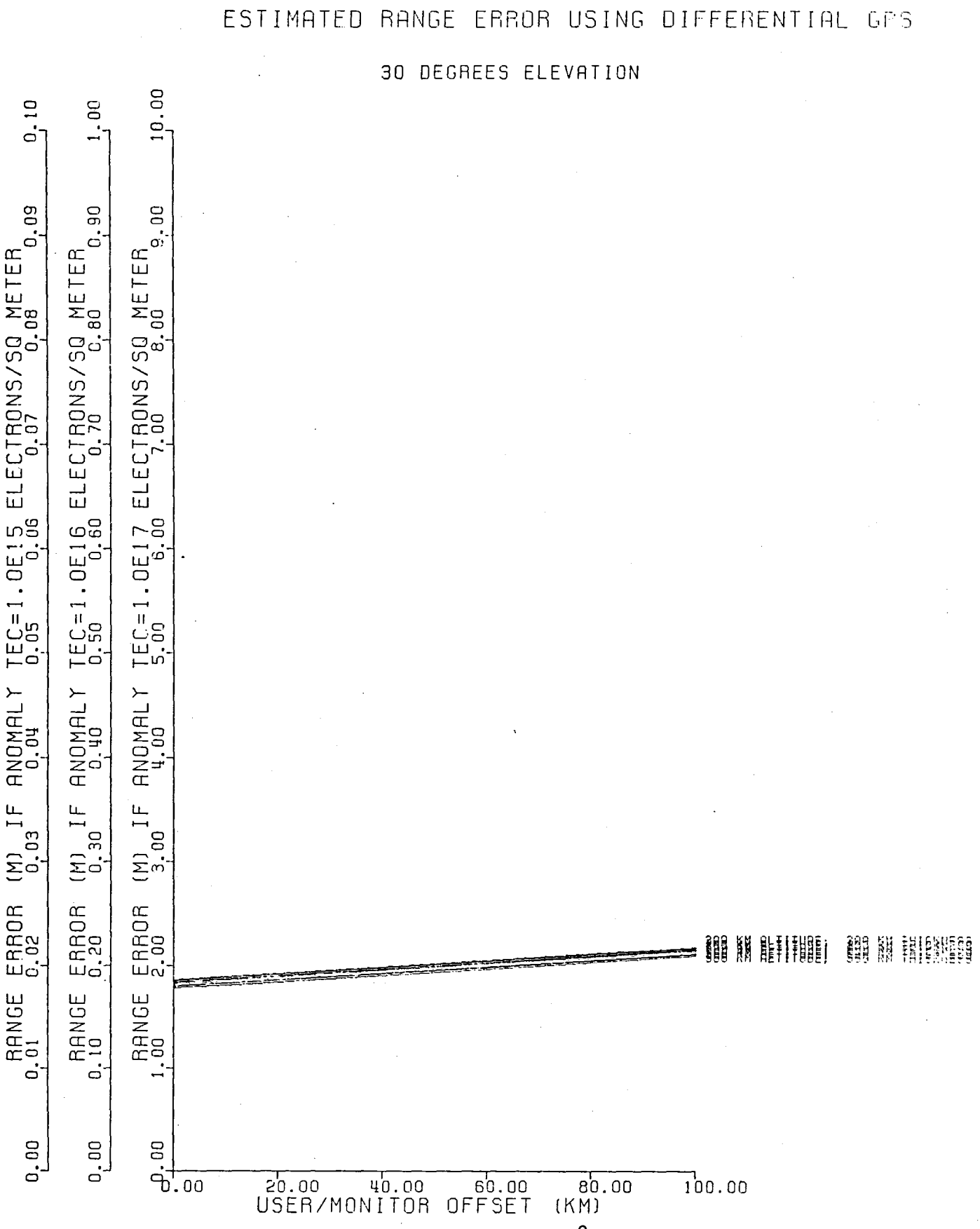

Figure 4-9. Range error at 30^{o} elevation.

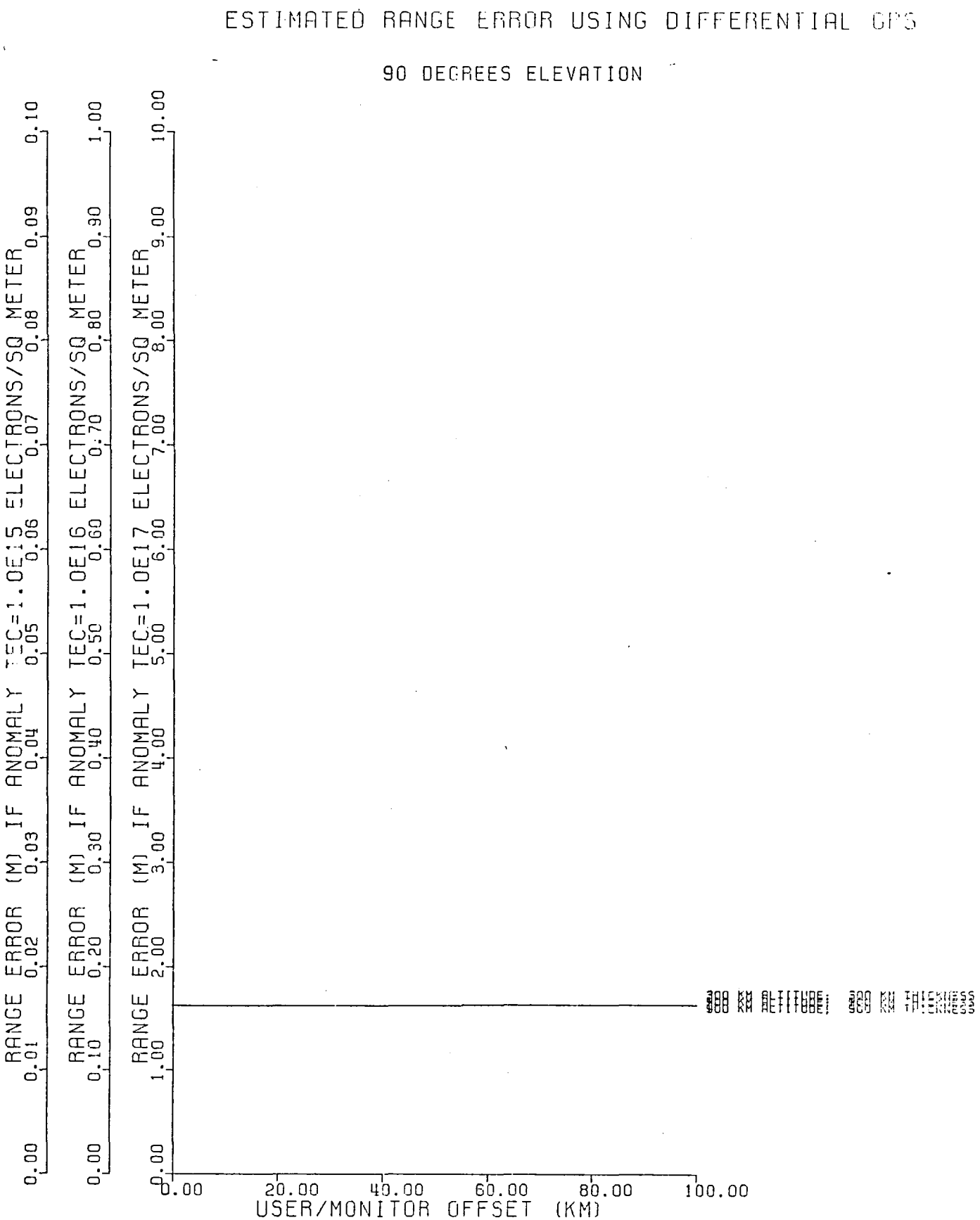

Figure 4-10. Range error at 90^{0} elevation.

4.5 Conclusion

To reiterate the observations regarding the previous discussion as outlined in the introduction to this section:

1. Range error is fairly insensitive to geometry (i.e., a factor of two over the cases examined).
2. The range error is linear with electron density.
3. The best results occur at 90^{o} elevation which is in concert with good vertical accuracies.
4. Nominal electron densities produce residual range error of less than one meter.

The conclusion then is that operation in a differential mode is feasible. A proof-of-concept experiment is therefore recommended.

5.0 DATA LINK REQUIREMENTS

5.1 Introduction

In order to assess the data link requirements in differential mode for support of collision avoidance and landing, a typical TCA scenario needs to be postulated. The scenario selected here is a mid-size air terminal with a major portion of its operations being general aviation. This is in contrast with high density terminals where nearly all operations are commercial. The latter choice would not be realistic in that the data link requirements which would result would not be representative of general aviation. A candidate terminal area which has the necessary mix of operations for proper analysis of data link requirements is the Raleigh-Durham airport in North Carolina.

Table 5-1 shows a forecast through 1990 of operations, general and commercial, for RDU as projected by the FAA [5-1]. The data shown in Table 5-1 are established by defining an operation to be that performed by aircraft that: 1) operate in the local traffic pattern within sight of the airport; 2) are known to be departing for, or arriving from, flights in local practice areas located within a twenty mile radius of the airport, or 3) execute simulated instrument approaches or low passes at the airport. An aircraft operation is counted for both a landing and a takeoff.

Table 5-1. Aviation Operations Forecast - RDU [5-1]
(In Thousands)

Year	Air Carrier	Transport and Commuter	General Aviation	Total*
1981	36	18	151	205
1982	37	19	152	205
1983	38	21	158	208
1984	38	22	161	217
1985	39	24	166	221
1986	40	24	179	243
1987	41	26	186	253
1988	41	27	193	261
1989	42	28	201	271
1990	43	30	209	282

*These values differ from those cited in [5-1] based on the above data in that they do not include a local and itinerant military aircraft. The differences are on the order of 5%, the above totals being low.

Using the 282 Kilo operations per year and assuming uniform distribution of operations throughout the year and traffic availability between 6:00 A.M. and 12:00 Midnight, one can calculate an hourly density of approximately 43 operations per hour. Assuming the coverage area to be the twenty mile radius given above, an aircraft at 175 knots spends approximately 7 minutes in the terminal area. This says that while any given aircraft is in the terminal area there is on the average 5 other aircraft under surveillance. Assuming that peak operations are an order-of-magnitude greater than the average and assuming a DABS link characteristic (i.e., 112 bit messages at a 4 Mbps rate), one could achieve approximately 1,400 two-way link operations with each aircraft every 4 seconds. This ignores guard bands for propagation delay but does demonstrate ample time for support of the collision avoidance aspects of the differential mode. This further implies that the actual link definition is probably dictated not by collision avoidance but by the demands of landing.

An aircraft during approach and landing at 100 knots traverses 169 feet a second. At the highest GPS update rate of 10 per second, the aircraft moves 16.9 feet between updates. The data link, to be effective during landing, should probably be capable of supporting a data rate based on this update rate (note that typical single and dual channel GPS receivers do not handle this rapid a solution rate - a difficulty to be resolved). With the assumptions stated above the link would have to provide round-trip messages to 50 aircraft every 0.1 second (this does not imply 50 aircraft landing simultaneous but simply guarantees homogeneity of the link over the ensemble of users). This results in a required link capacity of 500 messages per second. This says then that the data link poses no great problem with respect to capacity and in fact is compatible with DABS parameters.

5.2 TDMA Data Link

DABS has been selected for discussion above in that it is an in-place system and from an experimental or proof-of-concept-validation point-of-view is probably the most likely candidate for use with differential GPS. However, given that an idealistic desirable feature is operative without the need for ground-based instrumentation (other than the differential monitor), it becomes apparent that a TDMA structured link could perhaps more easily support the system. This idea gathers

more credance when it is remembered that the GPS clock could provide the synchronization which is an integral part of such a concept.

Toward this end it is appropriate to review the ANTC-117 standard for data links utilized in supporting Collision Avoidance systems, and to conceptualize a TDMA link. While the standard is directed at CAS, it is only a matter of message rate scaling to support landing functions. The following paragraphs pursue this concept.

Considerations for a TDMA Data Link

The following paragraphs describe relevant considerations of a TDMA data link to support a GPS based Collision Avoidance system. These were extracted from the ANTC-117 (Rev. 10, 1971) standard for TDMA links.

Communication Range:

[A-2-a-(1)] - ". . . detect all aircraft which present a potential danger."

[A-2-h-(5)] - Reliable communication range must be commensurate with speed capability and allow adequate time for "processing time, pilot and aircraft reaction times and obtaining of the required safe separation."

Capacity:

[A-2-d-(1)] - ". . . aircraft will be in line of sight of other participating aircraft in constantly varying quantity as high as at least 1,000 in number."

[A-2-f-(1)] - "To provide an acceptable system capacity margin for all airspace users, four frequencies . . . will generate 2,000 slots every three seconds."

Frequencies and Bandwidth:

[A-2-f-(1)] - "The center frequencies utilized are 1600 MHz, 1605 MHz, 1610 MHz, and 1615 MHz." Total band width is "from 1592.2 MHz to 1622.5 MHz."

Performance:

[A-2-h-(4)] - "The CAS must function in a normal manner during all in-flight maneuvers and in the presence of rough and smooth terrain, and man-made objects."

Protection Against Co-Slot Occupancy:

[B-1-c-(4)] - ". . . each aircraft system will stop transmitting and listen for one epoch in its own message slot on a random basis such that, on an average, co-slot occupancy is detected within forty seconds. Listening for co-slot occupancy should not occur during successive epochs nor during hazardous encounters until the encounter is past."

Protection From Line of Sight Interference

[B-1-d-(1)] - "A power budget analysis of a cooperating system designed to warn of a collision threat at 40 nm indicates that under some conditions . . . the system could possibly react to signals at six hundred miles."

[B-1-d-(2)] - Recommends "frequency shifting following the slot data period rather than increasing the slot period to include all or a portion of the line of sight transit time."

5.3 TDMA Data Link Characteristics

Information to be put on data link for the collision avoidance function:

Data	Bits (min-max)
Preamble	0 - 16
Position: x, y, z	48 - 60
Velocity: V_x, V_y, V_z	24 - 36
Identification	0 - 20
Capability	0 - 8
Maneuver intent	0 - 8
TOTAL	72 - 148

Total propagation and guard time required to protect against line of sight interference from range X:

X(nm)	Time(ms)
200	1.25
400	2.50
600	3.75

The amount of guard time required per slot can be reduced by using more than one frequency and shifting the frequency after each slot. However, the minimum propagation time per slot should be 1.25 mS, to allow detection of slot occupancy by an aircraft at a range of 200 miles or more.

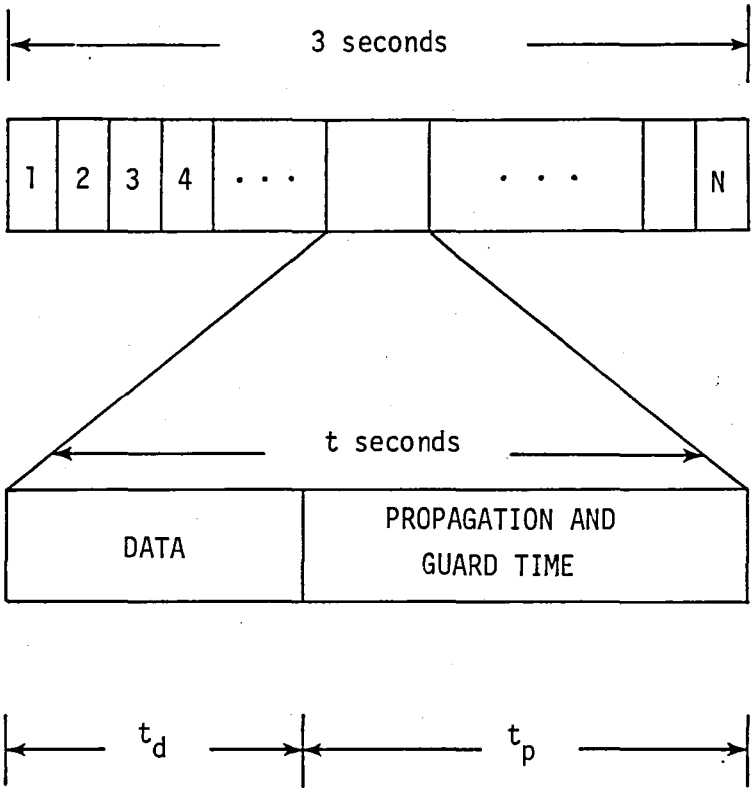

Figure 5-1. TDMA link message format.

The parameters and comments for the message format shown in figure 5-1 are discussed in the following paragraphs:

"N" is the number of time slots in the data link, or its maximum capacity. Its choice is affected by the communication range and the traffic density of the target period. A margin of additional slots helps to reduce the incidence of co-slot occupancy and associated problems. ANTC-117 suggests 2,000 slots.

"T" is the epoch length, or cycle time. Each aircraft will update and transmit its data once every T seconds. In choosing T, a trade-off is involved: a shorter period allows more frequent updating of threat evaluation parameters which increases accuracy and reduces the threat volume, while a longer period allows a lower data rate and/or more data and/or longer guard time. ANTC-117 suggests T=3 seconds when four frequencies are used. For a one-frequency system, guard time must be increased to protect against line of sight interference.

"t" is the length of each time slot, and is equal to T/N.

"t_d" is the period of time alloted for data transmission in each slot. The resulting data rate is b/t_d bps, where b is the number of bits in the data.

"t_p" is the combined propagation and guard time. It is the propagation delay from an aircraft at the desired maximum communication range plus additional time to guard against line of sight interference from aircraft at greater ranges which can occur due to fluctuations in the actual communication range. The necessary per slot guard time can be reduced by utilizing this technique, the entire subsequent slots which are on different frequencies can be considered to be part of the guard time. ANTC-117 suggests using four frequencies. The minimum reliable communication range should be at least 40 nm. ANTC-117 claims that a system designed for such a goal can produce line of sight interference from a range of 600 nm. "under some conditions". The probability of error in the received message from such line of sight interference as a function of guard time should be considered in choosing t_p and deciding whether the frequency shifting method is worth the extra cost and complexity it adds to the system.

6.0 USER EQUIPMENT DEFINITION

The user equipment shown in figure 6-1 is configured to support an experimental demonstration/evaluation program. Operational hardware would not include the instrumentation module. Dependent on the extent of processing specific to differential mode operation and data link forwarding which could be performed in the GPS receiver navigation processor the central processor could also be deleted. The control and display for an operational system would consist of a conventional GPS operator panel with the addition of those additional features necessary to establish the data link.

In the configuration shown, the central processor has a relatively simple role of forwarding collision avoidance information for input to the data link and of general interface with the display and control panel and with the instrumentation module. The level of sophistication of the processor is probably on the order of a DEC PDP 11/03 with limited memory running under the RT-11 operating system.

The control and display portion of the system consists of the normal GPS receiver controls and some technique for communication with the processor. A TI Silent 700 could provide this function and has the advantage of providing hard-copy output for in-flight documentation of test procedures.

The instrumentation envisioned consists of some technique for computer compatible mass storage such as a Kennedy Instrumental Tape Recorder and some form of strip chart recording for in-flight performance assessment. Parameters to be recorded include signal quality, position and velocity (either both before and after correction or corrected and correction factor), general housekeeping and flight documentation, and routine parameters from the normal flight instrumentation such as barometric pressure, etc.

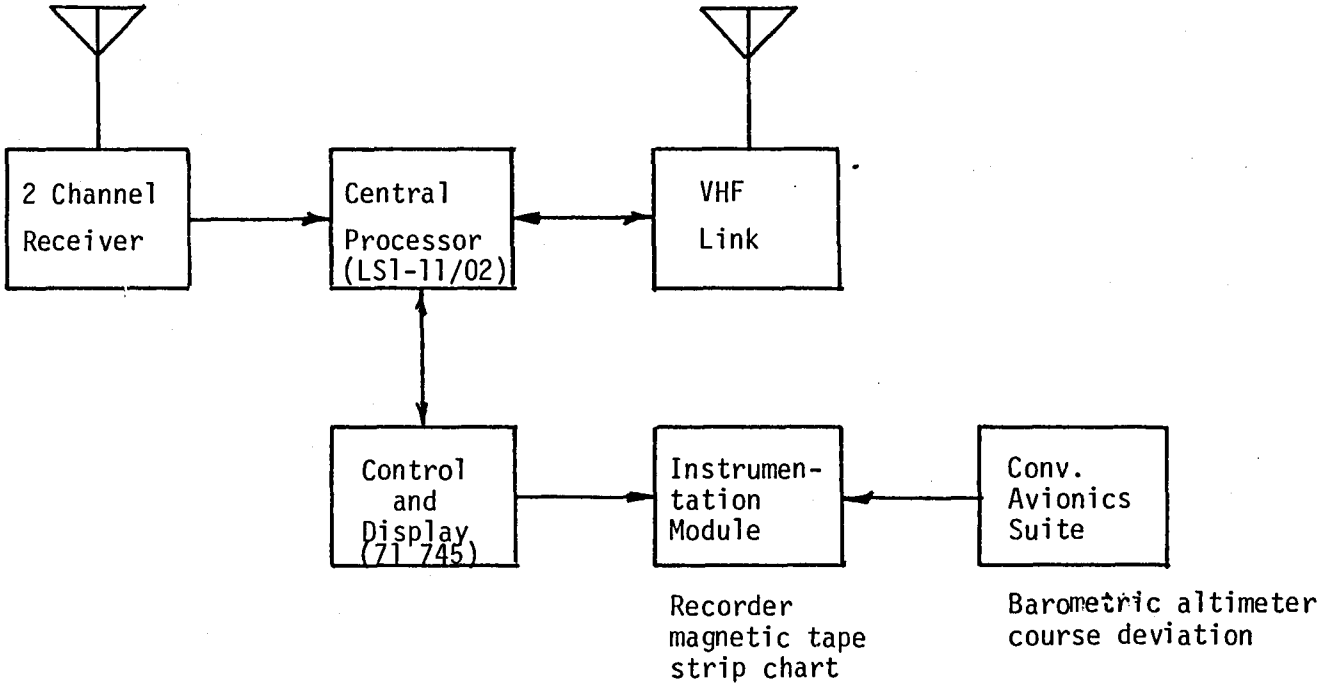

Figure 6-1. Conceptual user equipment configuration.

7.0 MONITOR STATION DEFINITION

The monitor station is configured with a four-channel receiver, VHF data link, and necessary instrumentation to support experimental verification. An important consideration is the receiver type selected for the monitor station. It is interesting to contrast whether the receiver should be as sophisticated as possible so as to account for the ionospheric propagation delay as accurately as possible or should resemble user equipment so as to calibrate out other uniform system errors. The latter was rejected as a possibility in that in general degraded performance would be encountered simply due to receiver design. With the four channel receiver, solutions from single frequency and dual frequency could be compared and the ionospheric delay uplinked directly to the user equipment.

Figure 7-1 indicates a candidate monitor station configuration. The emphasis has been placed on a station design which would support an experimental program rather than an operational configuration. It is anticipated that the station adopt the role of a laboratory and, as mentioned previously, be housed in a van to provide mobility both for experimental and logistical reasons.

The central processor provides the functions of data processing and system control. It is conceived to be a PDP-11/34 like minicomputer. It provides for such functions as signal quality monitoring, selection of differential or stand-alone operation, constellation prediction, data link formatting, etc. Interface between an instrumentation package and the central processor is provided by a control and display module. This module would implement the human interface with the machine providing digital readouts of selected parameters, keyboard interface, and possibly a CDTI display.

The instrumentation package provides two functions. The higher priority of the two being on-line mass storage of system performance. Data stored includes both system related and ancillary data. System related data includes traffic descriptive data such as arrival/departure time in TCA, flight profiles, time history of the correction vector, SNR time history, etc. Ancillary data required for performance interpretation includes such variables as wind speed and direction, temperature and humidity, barometric pressure, local time for general data synchronization, etc.

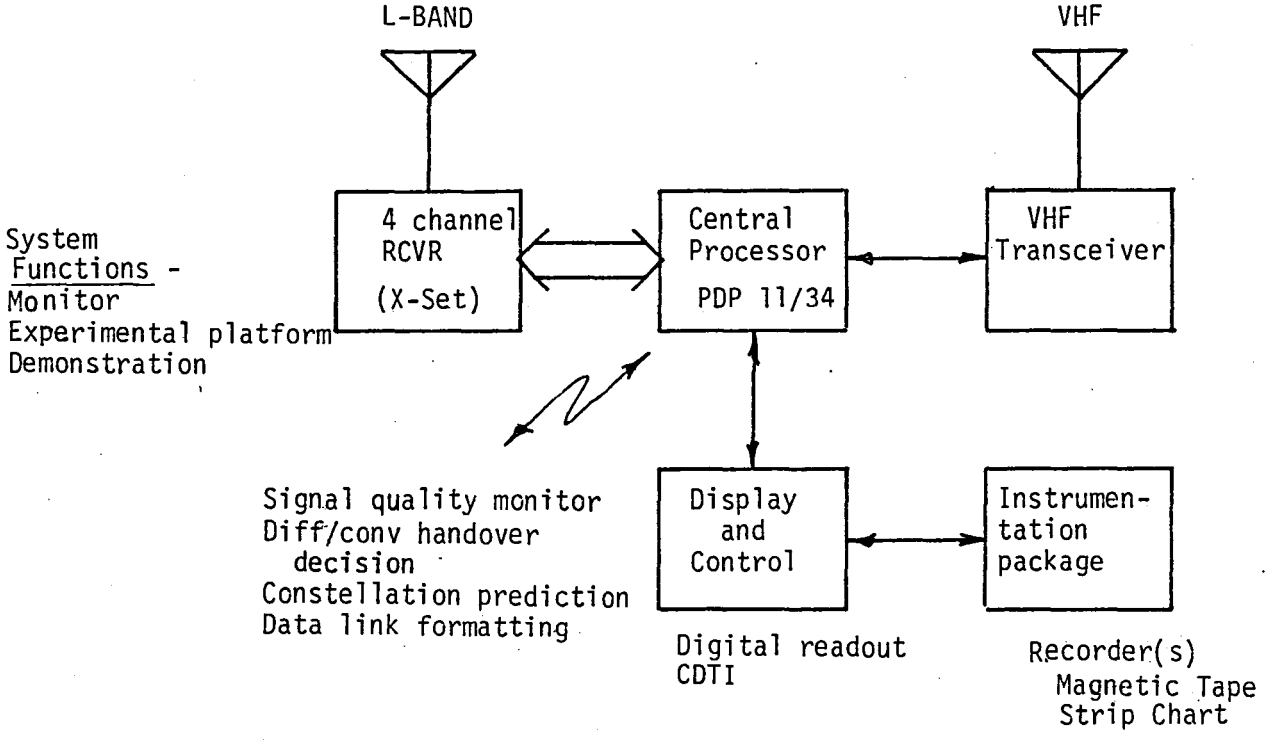

System Data -
- traffic -
- departure/arrival time in TCA
- correction vector
- correction vector time history
- SNR time history

Ancillary Data -
- wind speed and direction
- temperature
- humidity
- barometric pressure

Figure 7-1. Conceptual monitor configuration.

Data rates and volume are expected to be such that magnetic tape or floppy disk are viable cost-effective media. These also provide an easy media for transporting the data to other computational facilities. The inclusion of a strip chart recorder would be useful for on-site review of performance time histories.

It is anticipated that the monitor station generally be unattended but serviced (i.e. tapes changed, etc.) on a daily basis. During certain select experiment phases, operator presence would be desirable.

8.0 EXPERIMENT DESIGN

8.1 Introduction

This section presents a discussion of the elements of a proof-of-concept validation experiment. The discussion is relatively general although some quite specific issues are addressed and recommendations presented. Included is a statement of the issues defined for differential mode operation, functional definition of the experimental systems involved in the demonstration of landing and collision avoidance as derived from differential mode, and some further comments on the actual conduct of the evaluation/demonstration.

8.2 Differential GPS Experiment - Issues

The principal issues of the study can be loosely categorized into one of the following:

1) Correctability
2) Monitor Hardware
3) Data Format
4) User Processing
5) User Hardware

Each of these categories is treated in detail below.

Correctability

Among the various forms of error data that could be used (pseudo-range, position, ionospheric delay model), which correlates best with the data at the user's position and can be used conveniently for correction?

A remote user aircraft at ranges up to 150 km from the monitor must be simulated. This remote unit should include a representative general aviation GPS antenna, a high performance GPS receiver and a low cost GPS receiver. The pseudorange error, position error and ionospheric delay should be stored digitally on magnetic tape for later analysis. Signal-to-noise ratios should also be recorded. The same data are recorded simultaneously at the monitor location. Correlation studies should answer the question of which data about which satellites are to be transmitted. The

remote units would be situated at several ranges from the monitor and also at different headings from the monitor to determine the differential GPS monitor's coverage area.

The monitor's performance as a pseudolite at various ranges could also be tested.

Any factor which renders the monitor or user equipment inoperable or unreliable should be recorded with the error data. Such factors would include multipath, shading, noise, signal dropout or equipment failure.

Monitor Hardware

The simulated remotely-located aircraft could also be used as a test vehicle to determine optimum monitor location for reception and transmission (a separated transmitter and receiver could be tested; the receiver is positioned near the runway for terminal accuracy and the transmitter is at a distance to reduce interference and multipath and also to reduce dynamic range requirements for the differential link receiver).

Part 1 of the experiment will show whether a rotating directional antenna, transmitting bearing-dependent correction data, is worthwhile. If it is, this concept will be tested.

If the monitor is to be used as a pseudolite, a transmitting system for that purpose should be tested. The response pattern of the user's antenna would be a critical factor for this test.

Data Format

Other than the basic questions of waveband and encoding method, the important issue here is the update rate for each type of data transmitted. Part 1 of the study will determine what these are to be. The update rate must be high enough to retain good accuracy, but the user's update rate is not likely to be very high. The update rate should also be chosen to smooth the transition from a stand-alone mode and also that from one satellite constellation to another (if a satellite constellation is chosen; this seems very likely).

User Processing

Given that the nature and format of the data have been decided, the principal remaining problem is the user's transition protocol (stand-alone to differential mode, constellation to constellation, differential mode dropout).

The monitor and user will not always select the same constellation of 4 satellites, even if the choice is based solely upon GDoP. Thus, the user receiver may be required to accept a handover of data for a new constellation from the monitor. At the threshold of the coverage area, the user receiver should probably weight stand-alone data and differential data, so that simultaneous or alternating modes of operation are required.

While one constellation is being used, updates could be done as each satellite's pseudo-range is measured but if the constellation ranges, the pseudo-ranges for every satellite in the constellation must be determined before a fix is obtained (3 satellites might be used after acquisition).

The transition problem is alleviated if the user receiver is accepting only the parameters of an ionospheric model from the monitor to supplant those stored in the receiver. These parameters would not change as quickly as the pseudo-range or position corrections, and so could be used in case of monitor dropout. These ionospheric model data could be used at long ranges.

The test should determine whether stand-alone parameters can be conveniently overridden by signals from the monitor or directly by the user. The user update rate should also be examined.

Other possible add-ons to be tested are a Kalman filter to "track" satellites for improved accuracy and a weighting algorithm to minimize expected error at the boundary of the coverage area.

User Hardware

The items to be decided here are the receiver modifications required for differential-mode use, the display hardware and, especially, the satellite antenna and differential mode antenna design (to avoid dropouts).

The modifications must make the transition from stand-alone mode possible, but cost must be held to a minimum. A tradeoff may be necessary.

The display should be capable of indicating stand-alone and differential mode estimates of position in convenient units, so that malfunctions are easily recognized.

The antenna systems are expected to present a problem (dropouts, perhaps multipath, low signal-to-noise ratio for desired satellites etc.). Universality of the design is an important consideration.

8.3 Differential GPS Validation During Approach and Landing

Functional Definition

Figure 8-1 is a functional block diagram of a GPS -based guidance system for approach and landing. Note the high degree of commonality between this system and the GPS nagivation and collision avoidance functions. The same GPS receiver can be used for all three functions, and the data processing tasks required may share the same microprocessors and memory. Figure 8-2 illustrates one approach to designing the hardware for such an integrated system.

The operation of the approach and landing function is straightforward. The GPS receiver provides updates of the aircraft's position and velocity. These vectors are compared to a stored digital representation of the desired approach path. This path will have been computed from the desired approach profile and data specifying the exact location and orientation of the runway. These data can be transmitted to users via the same data link which provides differential GPS correction factors. The deviation from desired path is computed for each update of actual position, and this information is used to drive a display which commands the pilot to fly up, down, left, or right. Enough information is available to drive a more sophisticated display, if desired, but its cost would be prohibitive to most general aviation users.

The accuracy of this system depends not only on the accuracy of the GPS updates, but on the frequency with which the updates are provided as well. For the single-channel GPS receiver, the update rate is one per 3 seconds. In those three seconds, an aircraft travelling at 100 knots which is 3 degrees

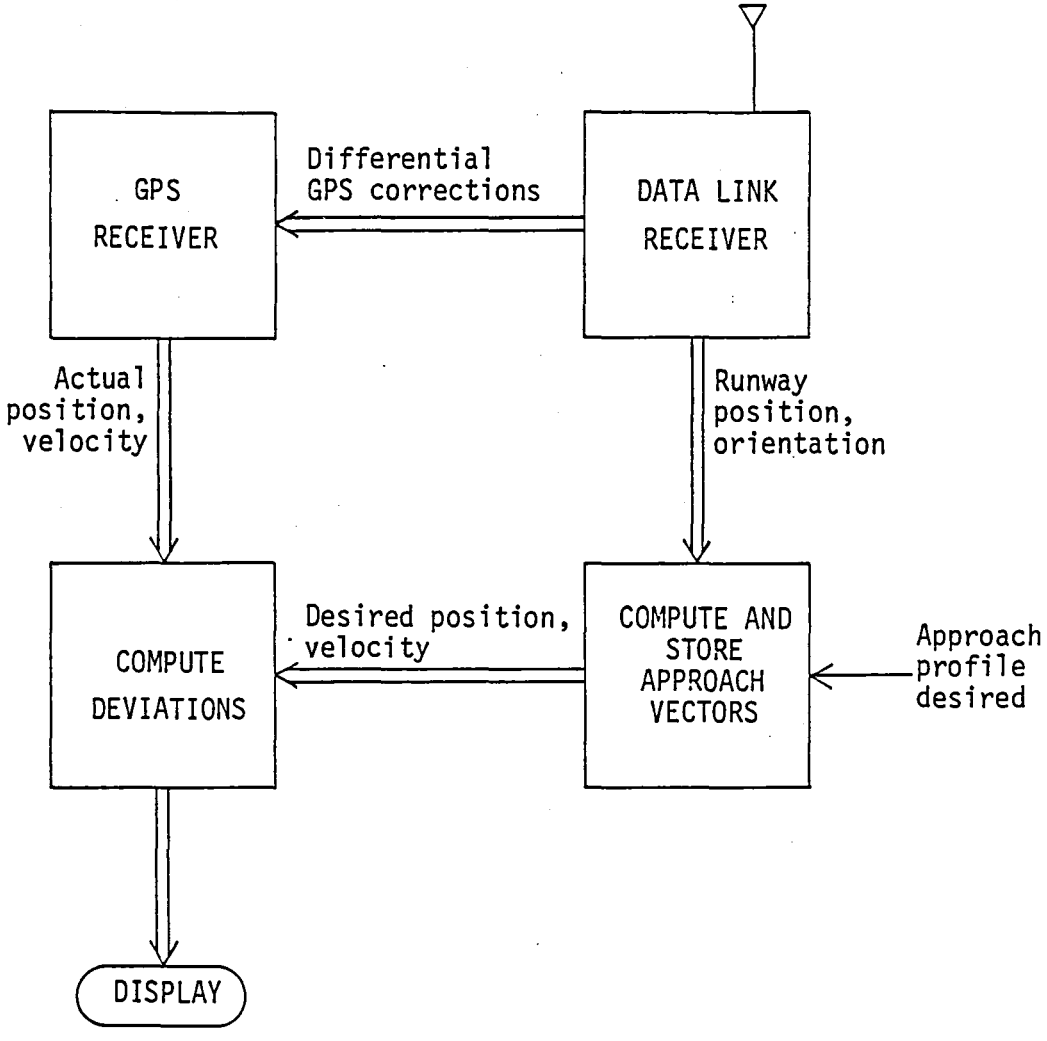

Figure 8-1. GPS based approach and landing system.

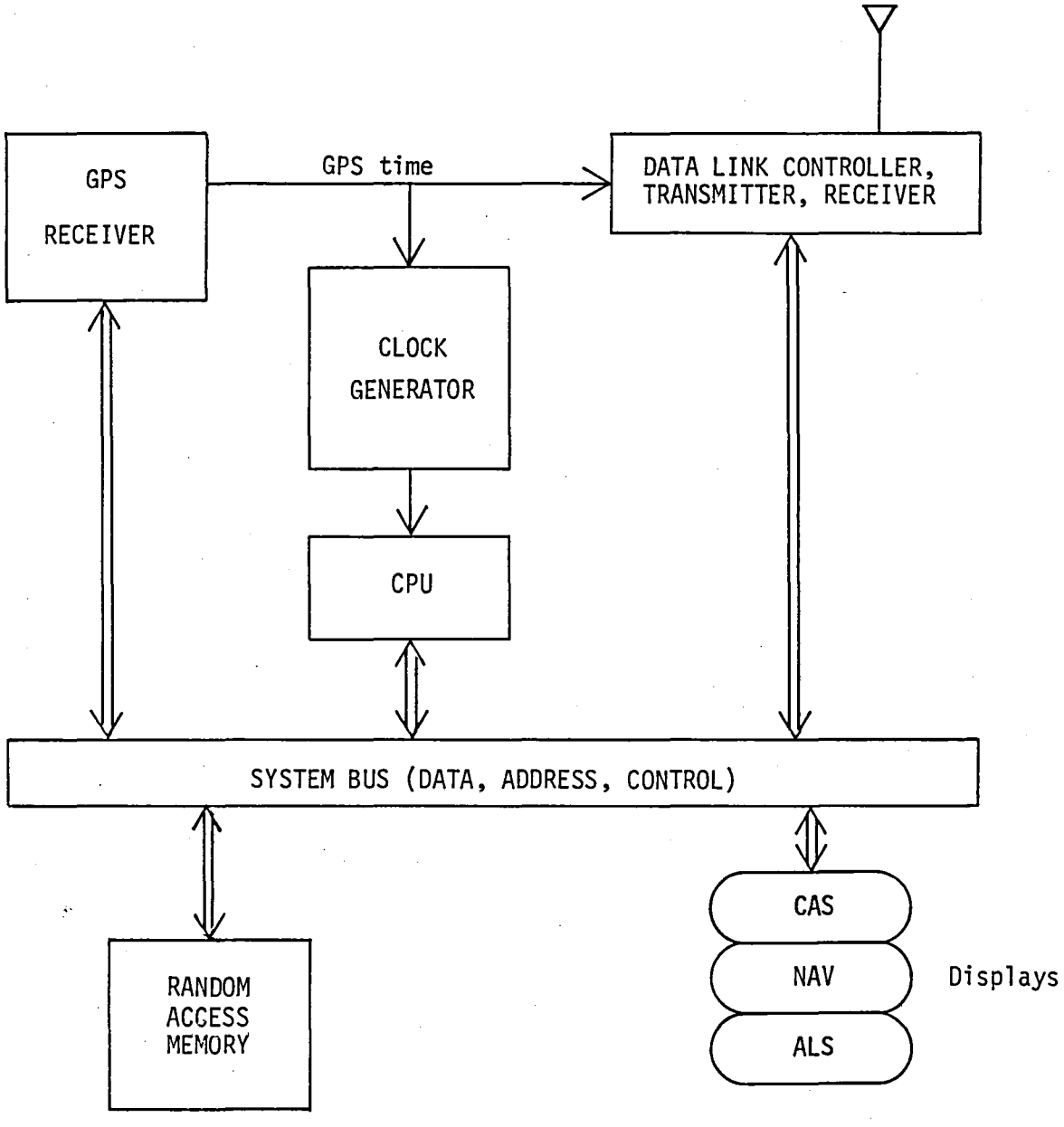

Figure 8-2. Integrated navigation, collision avoidance, and approach and landing system.

off course will drift 25 feet away from the desired path. While this degree of accuracy is sufficient for category II landings, it would be desirable to achieve a higher update rate for the purpose of presenting a smooth sequence of correction commands to the pilot. This can be accomplished by producing intermediate position updates computed by extrapolation of the previous vectors based on a constant acceleration assumption.

Experiment Concept

An experimental configuration to validate the concept of differential GPS for approach and landing should include the airborne experimental user equipment described in section 6 (see Figure 6-1), the experimental monitor station described in section 7 (see Figure 7-1), and a radar tracker at a research facility such as NASA-Wallops Island.

A key point in the conduct of these experiments is the ability to transition from stand-alone GPS to differential mode and on to one approach profile. Toward this end, all flight segments from enroute to approach should be exercised.

The procedure will consist of several approaches by the experiment aircraft, beginning from beyond the outer marker, and ending in a touch-and-go landing. Each of several approach profiles will be used, with the pilot navigating by stand-alone GPS to the start of each profile, then relying on the precision approach and landing system to guide the plan to the runway threshold (simulating a category II landing). Data will be recorded on tape throughout each sequence both in the airborne instrumentation module and in the ground station, as described in sections 6 and 7.

The post-experiment analysis will primarily compare the time histories of the aircraft's actual position (as measured by the radar tracking system) with those of the GPS-derived position, both before and after the transition to differential mode. The errors observed will be compared to predicted values, and to those permitted for a safe category II landing.

8.4 *Differential GPS Validation for Collision Avoidance System Functional Definition*

Figure 8-3 shows a functional block diagram of a GPS-based CAS for general aviation. The heart of this system is a low-cost GPS receiver of the "Spartan" type described in [8-1]. The salient features of this receiver are unaugmented accuracy in the range of 30 to 100 meters, time between updates of the navigation solution of 3 to 6 seconds, and time to first fix of approximately 2 minutes. Velocity is derived by differencing of successive position measurements. The output consists of three-dimensional position and velocity data in a convenient coordinate system, and precise GPS system time.

The position and velocity data is used by the threat evaluation subsystem and is transmitted to other aircraft (and possibly the ground-based ATC system) via the data link. The message to be transmitted is encoded by the message formatter, and may also include such additional information as identification, capability, and maneuver intent.

The operation of the transmitter and receiver is controlled by the data link control subsystem. If the data link utilized is of the TDMA type discussed earlier, the controller is responsible for the selection of a vacant time slot in which to transmit and implementation of schemes to minimize the likelihood of co-slot occupancy. It receives a signal from the receiver indicating whether or not the current time slot is occupied. Timing and synchronization is derived from the GPS system time output and is disseminated by the data link controller.

The receiver detects and decodes data transmitted by other aircraft or from the ground. Ground-transmitted messages may include differential GPS correction factors and automated warnings or advisories generated by the ATC system. In a TDMA data link, some time slots may be reserved for such messages to insure that they are not interfered with. When available, the differential GPS correction factors are sent to the GPS receiver for use in improving the accuracy of its position estimates. Error detection and correction may also be performed in the receiver section, if the design incorporates these features. If an uncorrectable error is detected, no data for that time slot is passed on.

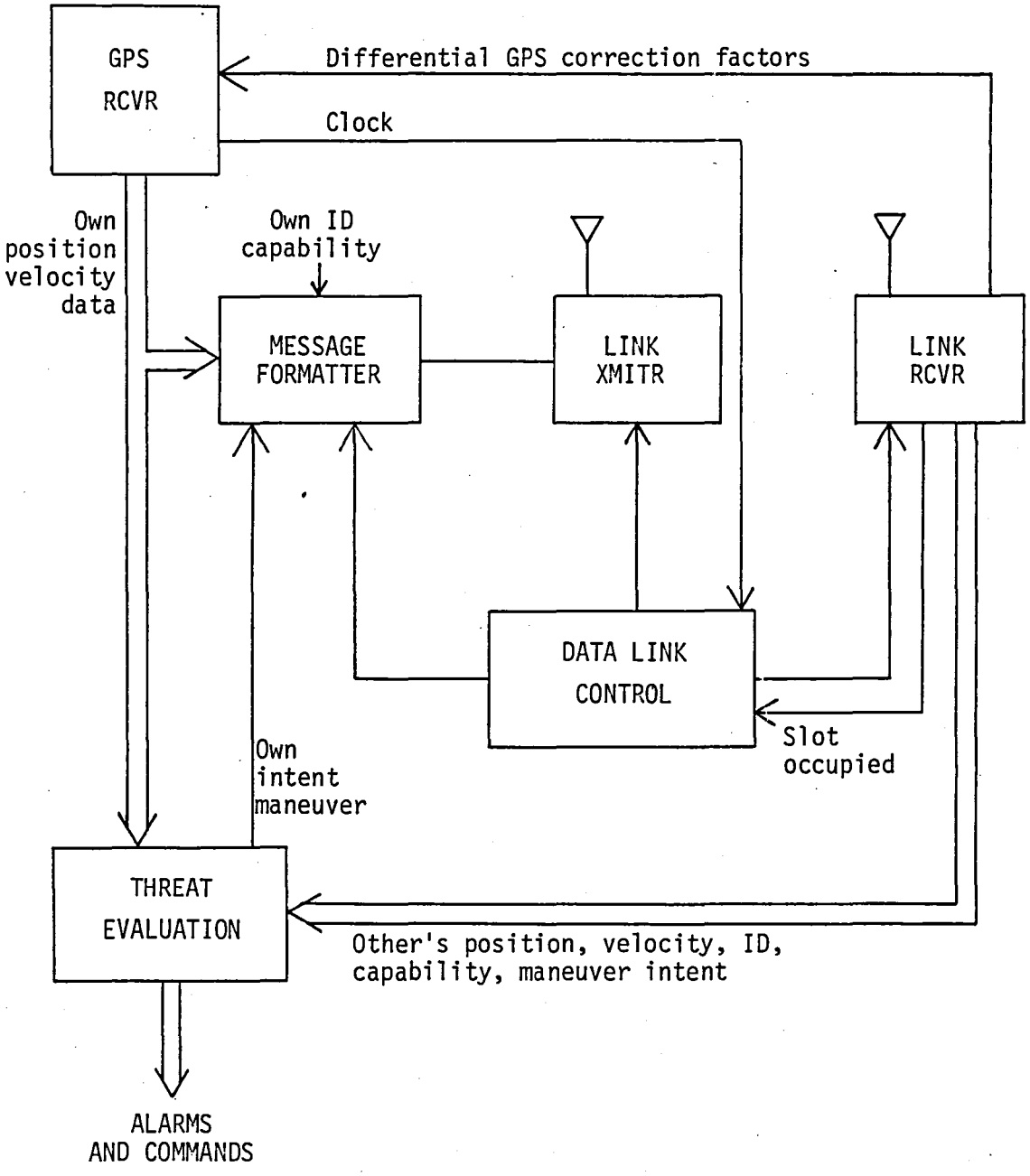

Figure 8-3 GPS based collision avoidance system.

Threat Evaluation

The threat evaluation subsystem is responsible for determining whether the aircraft is on a potential collision course and generating appropriate commands to the pilot for avoidance of the hazard when such potential exists. These commands may be positive or negative in nature, either requesting a maneuver in a particular direction (up, down, left or right) or specifying that a given maneuver must not be made. Most of the other independent-type collision avoidance systems can only issue vertical escape maneuvers, due to the fact that the only directional information available to them is the relative altitudes of the conflicting aircraft. However, in a GPS-based system, the precise positions and velocities of intruding aircraft are known. Thus, bearing and directional velocity information is available for use in selecting a more appropriate escape maneuver.

Threat evaluation will probably be implemented predominantly in software on a fast microprocessor system. This design will reduce costs and allow for easy implementation of automatic built-in test.

For each new set of data from the receiver, the collision potential is evaluated using the algorithm diagrammed in Figure 8-4. First, relative position and velocity vectors are computed by subtracting the corresponding absolute vectors. The magnitudes of these relative vectors are then computed, giving the relative range and range rate. The direction of each vector is also computed, giving the direction of the relative velocity and the bearing of the other aircraft. The relative range r and range rate $\dot{r}$ are tested using the "tau criterion" suggested by ANTC-117. If $r + \tau\dot{r} < R$, then a conflict has been detected. The parameter R is the minimum acceptable approach distance, and τ is a time constant which represents the warning time. This test simply determines whether or not the two planes in question will be closer than the distance R after τ seconds, if the present courses are maintained and accelerations are ignored. Since accelerations may exist and the velocities may be changing, the threat volume must be increased to allow for an extra margin of protection. In the algorithm discussed here, this is done by varying the parameter R. If the acceleration capabilities of the aircraft are available, this information can be used

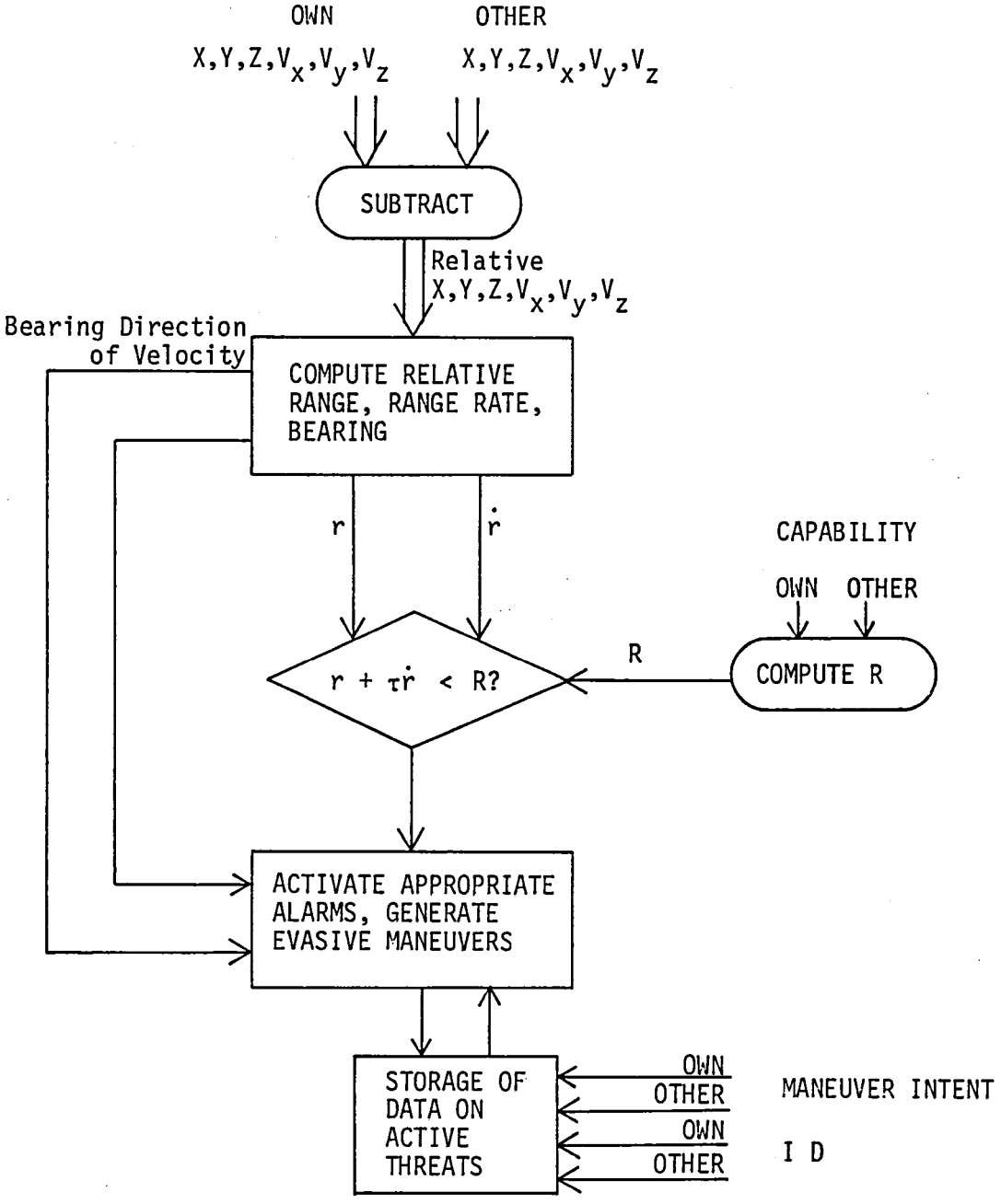

Figure 8-4. Threat evaluation logic.

to determine how much extra margin is needed. Thus, encounters with higher performance aircraft would result in greater threat volumes. The "capability" used for this purpose need not be the absolute maximum possible acceleration which the plane can attain but may be a limit to which the pilot will adhere, either by regulation or by convention. This limit may vary with altitude and location so that, for example, the terminal area limits would be more restrictive than elsewhere. Alternatively, the actual instantaneous accelerations of the aircraft could be measured and transmitted over the data link. This data could be used in the tau criterion test directly and only a minimal threat volume would be required. The net result of this extension would be to reduce the incidence of false alarms.

If it is determined that a collision threat exists, an appropriate command or evasive maneuver is issued to the pilot. In addition, data on the threatening aircraft is stored until the conflict is resolved. This is necessary for proper resolution of conflicts involving more than two planes. In selecting an evasive maneuver, the relative positions, velocities, and maneuver intents (if available) of all active threats are taken into account. In order to prevent aircraft involved in a conflict from maneuvering in such a way as to sustain the collision course, a "tie-breaking" decision can be made based on a comparison of the planes' identification codes and a predetermined convention. For example, in a two-plane encounter the one with the higher ID number might be designated as preferring "up" or "right" over "down" or "left" maneuvers when other factors do not render the decision unambiguous.

The output system for displaying commands to the pilot can be more or less sophisticated as cost dictates. Enough information is available to drive an elaborate traffic situation display if desired. However, a more appropriate display for a low-cost system might be similar to that proposed for the IPC function of DABS, shown in Figure 8-5.

Compatibility with Ground-Based Air Traffic Control

As described above, the GPS-based CAS with a TDMA data link is completely independent of the ground-based air traffic control system in its present form or that planned for the near-term future using DABS (Discrete

Address Beacon System). However, the addition of a monitoring facility on the ground to receive the messages on the TDMA data link would give the ATC system exact position data for all aircraft using the link, without having to interrogate them. This data could be used in the same way as position data derived from ATCRBS or DABS interrogations. Uplink messages which would otherwise be sent over the DABS ground-to-air data link could be put on the same TDMA data link, and would be displayed to the pilot if the GPS-CAS display unit is chosen to be compatible with DABS-IPC (intermittent positive control).

If total compatibility with DABS as presently envisioned is desired, the TDMA data link equipment can be replaced with data transceivers that would act like DABS transponders except that they could reply with position and velocity data instead of just altitude. When not in airspace controlled by a DABS sensor, the system could actively emit its own interrogations for performing collision avoidance, similar to the active BCAS system described previously. This technique would be more susceptible to garble, and would not take advantage of the precise time reference available to GPS users.

Experimental Concept

An experimental concept for flight validation is shown in Figure 8-6. Here again, the NASA-Wallops Research Runway Facility used in conjunction with the Terminal Air Traffic Model at NASA-Langley is considered as an ideal test configuration.

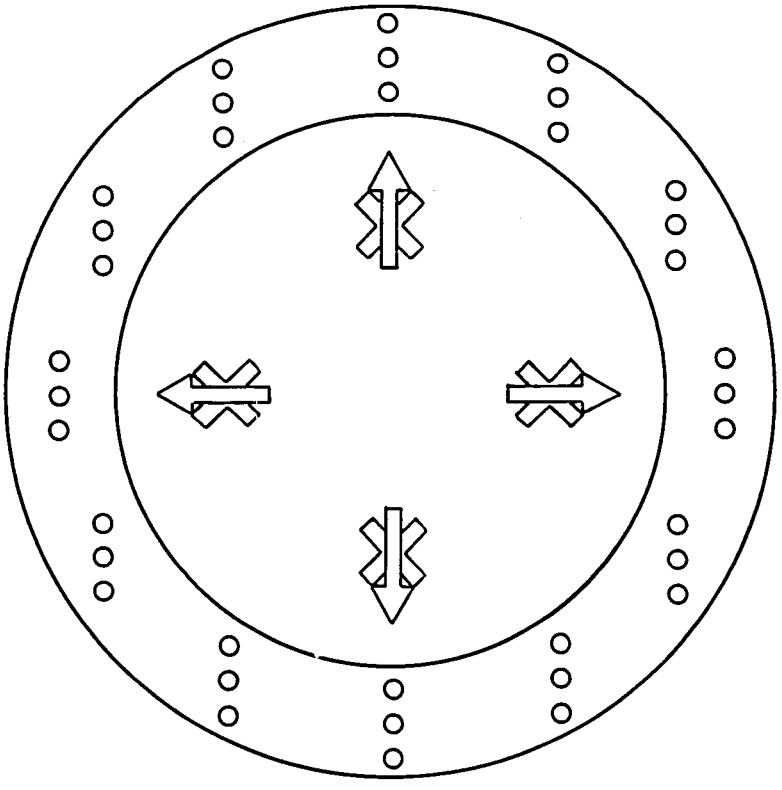

Figure 8-5. IPC Display

- A lighted arrow commonds a maneuver in that direction.
- A lighted "X" means "do not maneuver" in that direction.
- Bearing of intruding aircraft to the nearest 30 degrees ("clock system") is indicated by lights around perimeter.
- Relative altitude of intruder is indicated by which of the group of three lights is lit - above, below, or same level.

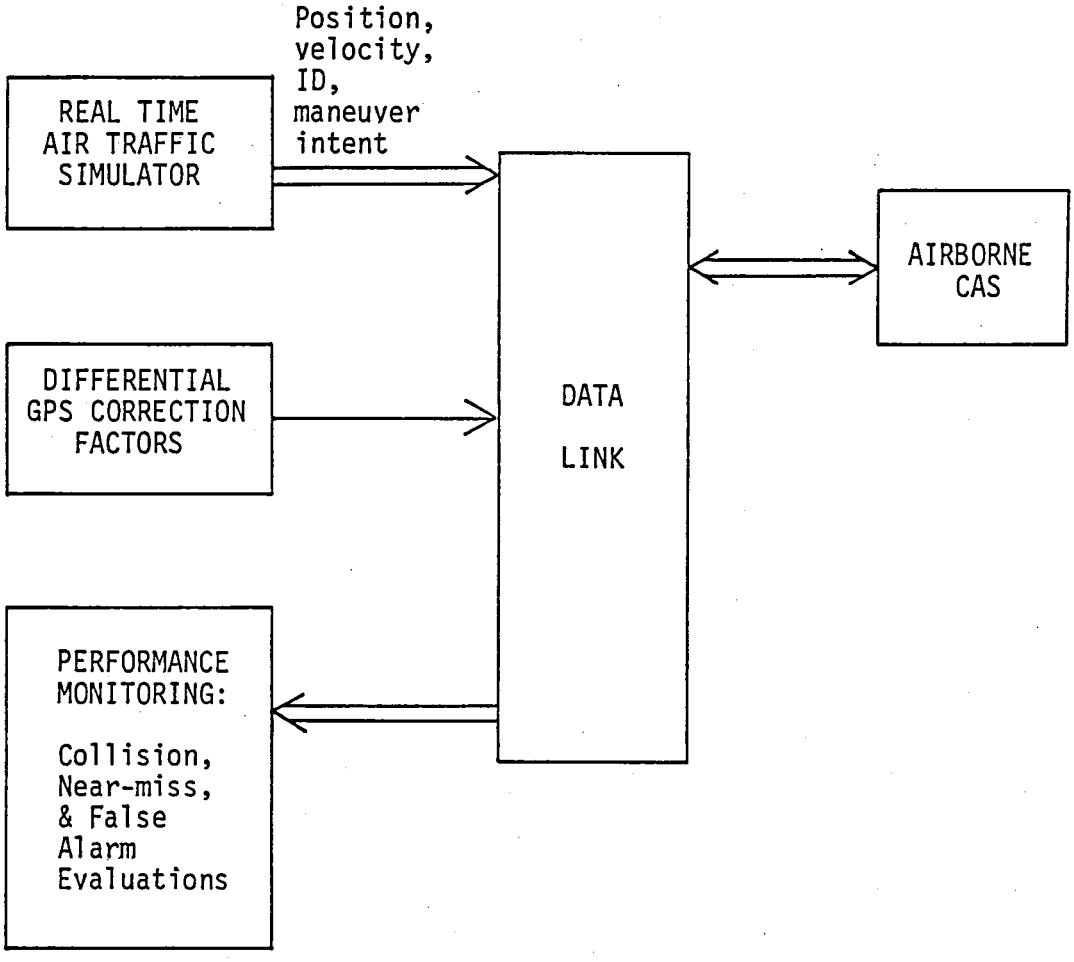

Figure 8-6. Experiment concept.

9.0 - REFERENCES

3-1 Alberts, R.D., and Ruedger, W.H., "Continued Study of NAVSTAR/GPS For General Aviation", RTI Final Report, RTI/1404/00-01 F (NASA CR 159145), December 1979.

3-2 Klobuchar, J.A., "Ionospheric Time Delay Corrections for Advanced Satellite Ranging Systems", AGARD Conference Proceedings on Propogation Limitations of Navigation and Positioning Systems, AGARD CP-209, Feb. 1977.

3-3 "Global Positioning System (GPS) Final Report, Part II - Volume B, User Segment Trades and Analyses" Philco-Ford Corporation, Report No. SAMSO TR 74-183, February 28, 1974.

3-4 Martin, E.H., "GPS User Equipment Error Models", Navigation, Journal of the ION, Vol. 25, No. 2, Summer 1978.

4-1 Hinder, R. and M. Ryle, "Atmospheric Limitations to the Angular Resolution of Aperture Synthesis Radio Telescopes", Mon. Not. Roy. Astron. Soc., 154, 229-253.

4-2 Philco-Ford, "Global Pos. System-Final Rept.", pt. II, Vol. A, 28 Feb. 1974, DDC No. AD921755, p. 5-5.

4-3 Titheridge, J. E., "The characteristics of large ionospheric irregularities", J. Atmos. & Terr. Phys., 30, (1968), pp. 73-84.

4-4 Garriott, O. K., A. V. daRosa, Jr., W. T. Ross, "Electron content obtained from Faraday rotation and phase path length variations", J. Atmos. Terr. Phys., 32, pp. 705-727.

4-5 Chan, K. L. and O. G. Villard, Jr., "Observation of Large-Scale Traveling Ionospheric Disturbances by Spaced-Path High Frequency Instantaneous-Frequency Measurements", J. Geophys. Res., 67, No. 3, (1962), p. 973-988.

4-6 Warwick, R. S., R. J. Davis and R. E. Spencer, "Phase stability angular structure and position measurement with a radio-link interferometer", Mon. Not. Roy. Astron. Soc., 177, 335,347.

4-7 Hamaker, J. P., "Atmospheric delay fluctuations with scale sizes greater than one kilometer", Radio Science, 13, 5, pp. 873-891.

4-8 Martyn, D. F., "Normal F region of the ionosphere", Proc. IRE, 47, Feb. 1959, pp. 147-155.

4-9 Hewish, A., "The diffraction of galactic radio waves as a method of investigating structure of the ionosphere", Proc. Roy. Soc. London, A-214, (1952), pp. 494-514.

4-10 Chan, K. L. and O. G. Villard, Jr., "Observation of Large-Scale Traveling Ionospheric Disturbances by Spaced-Path High-Frequency Instantaneous-Frequency Measurements", J. of Geophys. Res., 67, (1962), p. 973.

4-11 Munro, G. H., "Travelling disturbances in the ionosphere", Proc. Roy. Soc. London, A-202, (1950), p. 208.

4-12 Munro, G. H., "Travelling Ionospheric Disturbances in the F Region", Australian Journal of Physics, 11, (1957), p. 91.

4-13 Maxwell, A. and C. G. Little, "A Radio-Astronomical Investigation of Winds in the Upper Atmosphere", Nature, 169, (1952), p. 746.

4-14 Maxwell, A. and M. Dagg, "A Radio Astronomical Investigation of Drift Movements in the Upper Atmosphere", Phil. Mag., Ser. 7, Vol. 45, No. 365, (1954), p. 551.

4-15 Johnson, F. S. (Ed), Satellite Environment Handbook, Stanford University Press, Stanford, California, Chapter 2.

4-16 Garriott, O. K., A. V. da Rosa, M. J. Davis and O. G. Villard, "Solar Flare Effects in the Ionosphere", J. Geophys. Res., 72, (1967), p. 6099.

4-17 Hecht, Eugene and Alfred Zajac, Optics, Addison-Wesley, p. 87.

4-18 Hecht, Eugene and Alfred Zajac, Optics, Addison-Wesley, p. 205.

4-19 Klabuchar and Johanson, "Correlation Distance of Mean Daytime Electron Content".

5-1 Kruisic, P.G., Henry, T.E., Wine, C.R, "Terminal Area Forcasts: Fiscal Years 1979-1980", FAA-AVP-78-6, June 1978.

8-1 Magnavox, "Design Development Study for the Global Positioning System Spartan Set", MRL-85001042, 4 September 1975.

APPENDIX A - PHASE and GROUP VELOCITY

A.1 PHASE AND GROUP VELOCITY

The ionosphere is a plasma. Propagation of electromagnetic radiation is influenced by the presence of free (unbound) electrons. The more massive positive ions have little effect. The ratio of the speed of light in vacuo, c, to the phase velocity, v_p, is the index of refraction, n, and is given by

$$n^2 = 1 - (\omega_{p/\omega})^2 \quad [17]$$

where ω_p is the plasma frequency

$$\omega^2_p = Ne^2/\varepsilon_o m_e$$

where N = number density of electrons
e = charge on the electron
ε_o = permittivity of free space
m_e = mass of the electron

The phase velocity is thus greater than c.

Group velocity, v_g, can be determined from the relationship [18]

$$v_g = v_p + k\frac{dv_p}{dk}$$

where $k = 2\pi\ \lambda$
λ is the wavelength

Since $\omega = kc/n$, the above becomes

$$v_g = v_p\left(1 - \frac{k}{n}\frac{dn}{dk}\right)$$

furthermore by substituting

$$\frac{dn}{dk} = \frac{dn}{d\omega} \cdot \frac{d\omega}{dk}.$$

and

$$\frac{d\omega}{dk} = c/n$$

one obtains

$$v_g = v_p\left(1 - \frac{\omega}{n}\frac{dn}{d\omega}\right),$$

an expression as a function of ω.

The terms n and v will be expressed as functions of ω, manipulations made and the bionomial expansion applied to show the relation between v_g and v_p. Thus,

$$v_g = \frac{c}{\left(1-\left(\omega_{p/\omega}\right)^2\right)^{1/2}} \cdot \left[1 - \frac{\omega}{\left(1-\omega^2{}_{p/\omega^2}\right)^{1/2}} \cdot \frac{\omega^2{}_{p/\omega^3}}{\left(1-\omega^2{}_{p/\omega^2}\right)^{1/2}}\right]$$

becomes

$$v_g = \frac{c\left(1 - 2\left(\frac{\omega_p}{\omega}\right)^2\right)}{\left(1 - \left(\omega_{p/\omega}\right)^2\right)^{3/2}}.$$

Now for $\omega_{p/\omega} \ll 1$

$$v_g = c\left(1 - 2\left(\omega_{p/\omega}\right)^2\right)\left(1 + \frac{3}{2}\left(\frac{\omega_p}{\omega}\right)^2 - \ldots\right).$$

Multiplying and discarding terms in $\left({}^{\omega}p/_{\omega}\right)^4$ and above:

$$v_g \approx c\left(1 - \frac{4}{2}\left({}^{\omega}p/_{\omega}\right)^2 + {}^{3}/_{2}\left(\frac{\omega_p}{\omega}\right)^2\right)$$

$$v_g \approx c\left(1 - \frac{1}{2}\left({}^{\omega}p/_{\omega}\right)^2\right).$$

Expression for phase velocity must be expanded in the same way for comparison.

Since

$$v_p = c\left(1 - \left({}^{\omega}p/_{\omega}\right)^2\right)^{-1/2}$$

$$v_p \approx c\left(1 + \frac{1}{2}\left(\frac{\omega_p}{\omega}\right)^2\right).$$

Thus, it is seen that the group velocity is less than c by the same amount, $1/2\left(\frac{\omega_p}{\omega}\right)^2$, that the phase velocity is greater than c when ${}^{\omega}p/_{\omega} << 1$. Electron densities sometimes reach 2.5×10^5 electrons/cm^3 [8] giving a maximum ω_p of 28×10^6/sec. L band frequencies are on the order of $2\pi \times 10^9$/sec making ${}^{\omega}p/_{\omega} \approx 2 \times 10^{-5}$, thus the above results are very good approximations.

APPENDIX B - DEDUCTION OF TOTAL VERTICAL CONTENT FROM MAXIMUM ELECTRON DENSITY

B.1 RATIO OF MAXIMUM DENSITY AND TOTAL CONTENT

Graphs of electron density as a function of altitude are published in the Satellite Environment Handbook [4-15]. There are density profiles for night and day, high and low solar activity, up to 1000 km. Electron density above 1000 km could be estimated by an exponential function which fits very well the portion of profile above 600 km. Maximum densities were read from the profiles and are displayed in the first table. Results of the integration of the exponential function added to the numeric integration of the rest of the profile are given in the second table. The ratio of these total columnar integrated contents to the maximum densities are displayed in the third table.

TABLE B-1 - Maximum Density (10^5 electrons/cm^3)

solar activity/	day	night
high	20	4.5
low	5	1.9

TABLE B-2 - Integrated Content (10^{17} electrons/m^2)

high	6.4	1.16
low	1.2	.33

TABLE B-3 - Ratio Total Content/Density $\left(10^{11} \frac{cm^3}{m^2}\right)$

high	3.2	2.6
low	2.4	1.8

The ratios in the third table differ by less than a factor of 2 although total content varies by a factor of nearly 20.

At high solar activity, the ratio varies less than 25%. This would seem to imply that use of the ratio 3.2 x 10^{11} $cm^3/_m2$ could give total content from electron density maps at high solar activity with an error less than 25% at any time of day with accuracy improving the closer one is to noontime conditions.

B.2 MAPS OF f_0F_2 AND MAXIMUM GRADIENT

D. F. Martyn in his review "The Normal F Region of the Ionosphere" [4-8] has reproduced from an earlier paper world contours of f_0F_2 for maximum and minimum sunspot activity, equinox and solstice months. He states that peak electron density is given by $N_m = 1.24(f_0)^2 \times 10^4$ electrons/$cm^3(MHz)^2$. The $f_0 = 8$ and $f_0 = 10$ contours come very close together in Figure 2 of that paper (1947 Equinox) at the geomagnetic equator at about 6:15 local time. The difference in local time is about 17 minutes. The respective maximum densities are 7.9 x 10^5 and 12.4 x 10^5 electrons/cm^3. Using the previously defined ratio 3.2 x 10^{11} cm^3/m^2 gives respective columnar contents of 2.5 x 10^{17} and 4.0 x 10^{17} electrons/m^2 for an approximate change of 1.5 x 10^{17} electrons/m^2 in 17 minutes. This is 1.4 x 10^{14} electrons/m^2/sec, or about 4 mm/sec range change at 1.23GHz.

The speed of rotation at the equator is .465 km/sec. This implies a horizontal gradient of 3 x 10^{14} electrons/km or 8.6 mm/km.

These gradients are very large and comparable to maxima calculated for ionospheric disturbances of various types. This exercise is, however, susceptible to errors from many sources. The contours are drawn from data from 64 observatories and may not be accurate in the detail they may imply. The content to density ratio is uncertain to at best 10%. The contour measurements themselves are subject to irregularities in the F region, which have a relation to total content, but do not determine it completely or linearly as was herein assumed.

This exercise is useful in estimating maximum gradients which may exist. It is notable that the rates and gradients found are not greater than those found by other methods.

APPENDIX C - PATH LENGTH THROUGH THE IONOSPHERE AS A FUNCTION OF ZENITH ANGLE

For this purpose, the ionosphere will be modelled as a spherical shell of thickness t situated at a height h above the surface of the earth. In Figure 1 the observer is located on the surface of the earth at O. The radius from the center of the earth is drawn to him as are radii to the point of incidence of his line of sight on the bottom of the ionosphere and the point of incidence on the top of the ionosphere. The path length BT is found by finding angles i, β and c_2 as a function of the zenith angle z. Angle i is found by applying the law of sines to triangle OCB as is β in triangle OCT:

$$\frac{\sin(180° - z)}{(R + h)} = \frac{\sin i}{R}$$

or

$$\frac{\sin z}{(R + h)} = \frac{\sin i}{R} \quad .$$

Likewise

$$\frac{\sin z}{(R + h + t)} = \frac{\sin \beta}{R}$$

Angle c_2 in triangle BCT is $180° - (180°-i) - B = i - B$.
Length BT is then given by the law of sines

$$\frac{BT}{\sin c_2} = \frac{R + h}{\sin \beta} \quad .$$

The obliquity factor is the ratio of path BT to the thickness t. The secant of angle i is a good approximation to the obliquity factor and would obtain if the thickness were zero. However, the thickness and the curvature of the top of the ionosphere reduces the path length from that

computed using secant i. The angles i, β and c_2, secant i, path length and obliquity factor are given in the tables as a function of zenith angle. These are computed for thickness = 200 km and height = 300 km and also height = 250 km, which may be a better approximation [4-8].

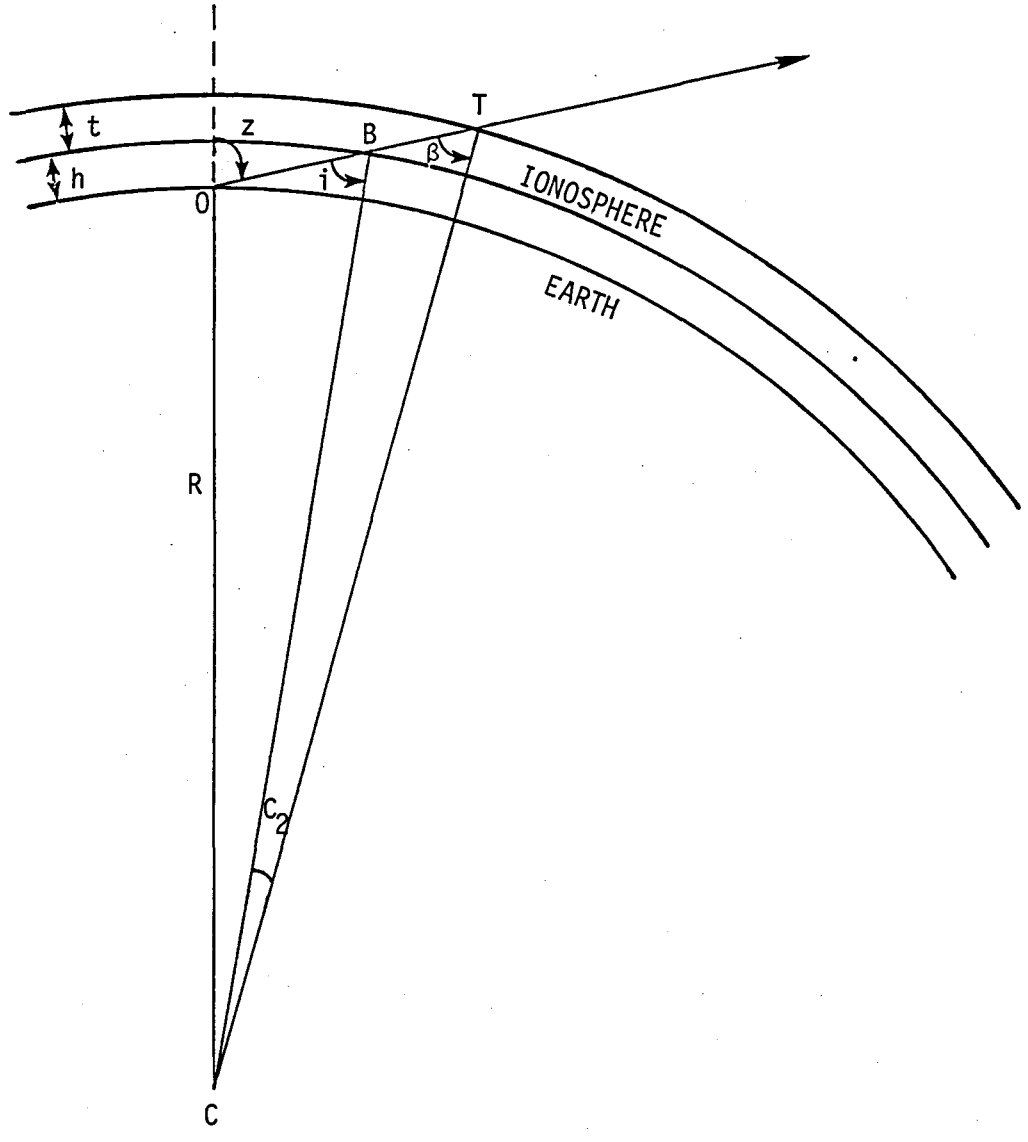

Figure C-1. Geometrical factors for computation of ionospheric path length.

TABLE C-1

Path Length Geometry For Height = 300 km, Thickness = 200 km

z	Angles in Degrees i	β	c_2	sec i	path (km)	obliquity
30	28.5	27.6	.903	1.14	227	1.13
45	42.5	41.0	1.509	1.36	268	1.34
60	55.8	53.4	2.382	1.78	345	1.73
70	63.8	60.6	3.211	2.27	429	2.14
80	70.1	65.9	4.196	2.94	534	2.67
85	72.1	67.5	4.589	3.25	578	2.89
90	72.8	68.0	4.745	3.37	595	2.97

TABLE C-2

Path Length Geometry For Height = 250 km, Thickness = 200 km

z	Angles in Degrees i	β	c_2	sec i	path (km)	obliquity
30	28.8	27.8	.918	1.14	227	1.14
45	42.9	41.3	1.541	1.36	270	1.35
60	56.4	54.0	2.454	1.81	350	1.75
70	64.7	61.4	3.351	2.34	441	2.20
80	71.4	66.9	4.472	3.13	561	2.81
85	73.5	68.5	4.943	3.51	613	3.07
90	74.2	69.1	5.133	3.67	634	3.17

APPENDIX D - TABULAR SIMULATION RESULTS

Table D-1, Simulation Results for 100 Km Altitude and 100 Km Thickness

TEC*	OFFSET in Km	ELEVATION in Degrees	RANGE ERROR in Km
1.0E+15	0.0	90	0.016
1.0E+15	0.0	30	0.019
1.0E+15	0.0	10	0.060
1.0E+15	0.0	5	0.072
1.0E+15	10.0	90	0.016
1.0E+15	10.0	30	0.047
1.0E+15	10.0	10	0.160
1.0E+15	10.0	5	0.135
1.0E+15	100.0	90	0.022
1.0E+15	100.0	30	0.312
1.0E+15	100.0	10	1.044
1.0E+15	100.0	5	0.664
1.0E+16	0.0	90	0.162
1.0E+16	0.0	30	0.186
1.0E+16	0.0	10	0.599
1.0E+16	0.0	5	0.715
1.0E+16	10.0	90	0.163
1.0E+16	10.0	30	0.215
1.0E+16	10.0	10	0.702
1.0E+16	10.0	5	0.781
1.0E+16	100.0	90	0.168
1.0E+16	100.0	30	0.481
1.0E+16	100.0	10	1.604
1.0E+16	100.0	5	1.323
1.5E+17	0.0	90	2.437
1.5E+17	0.0	30	2.793
1.5E+17	0.0	10	8.993
1.5E+17	0.0	5	10.733
1.5E+17	10.0	90	2.437
1.5E+17	10.0	30	2.825
1.5E+17	10.0	10	9.126
1.5E+17	10.0	5	10.825
1.5E+17	100.0	90	2.444
1.5E+17	100.0	30	3.120
1.5E+17	100.0	10	10.313
1.5E+17	100.0	5	11.593

* TEC-Total Electron Content.

Table D-2, Simulation Results for 100 Km Altitude and 300 Km Thickness

TEC*	OFFSET in Km	ELEVATION in Degrees	RANGE ERROR in Km
1.0E+15	0.0	90	0.016
1.0E+15	0.0	30	0.019
1.0E+15	0.0	10	0.052
1.0E+15	0.0	5	0.059
1.0E+15	10.0	90	0.016
1.0E+15	10.0	30	0.047
1.0E+15	10.0	10	0.152
1.0E+15	10.0	5	0.123
1.0E+15	100.0	90	0.022
1.0E+15	100.0	30	0.312
1.0E+15	100.0	10	1.035
1.0E+15	100.0	5	0.651
1.0E+16	0.0	90	0.162
1.0E+16	0.0	30	0.185
1.0E+16	0.0	10	0.521
1.0E+16	0.0	5	0.595
1.0E+16	10.0	90	0.163
1.0E+16	10.0	30	0.214
1.0E+16	10.0	10	0.623
1.0E+16	10.0	5	0.659
1.0E+16	100.0	90	0.168
1.0E+16	100.0	30	0.480
1.0E+16	100.0	10	1.518
1.0E+16	100.0	5	1.196
1.5E+17	0.0	90	2.437
1.5E+17	0.0	30	2.781
1.5E+17	0.0	10	7.821
1.5E+17	0.0	5	8.922
1.5E+17	10.0	90	2.438
1.5E+17	10.0	30	2.813
1.5E+17	10.0	10	7.943
1.5E+17	10.0	5	9.002
1.5E+17	100.0	90	2.444
1.5E+17	100.0	30	3.106
1.5E+17	100.0	10	9.026
1.5E+17	100.0	5	9.672

* TEC-Total Electron Content.

Table D-3, Simulation Results for 100 Km Altitude and 900 Km Thickness

TEC*	OFFSET in Km	ELEVATION in Degrees	RANGE ERROR in Km
1.0E+15	0.0	90	0.016
1.0E+15	0.0	30	0.018
1.0E+15	0.0	10	0.041
1.0E+15	0.0	5	0.045
1.0E+15	10.0	90	0.016
1.0E+15	10.0	30	0.047
1.0E+15	10.0	10	0.141
1.0E+15	10.0	5	0.109
1.0E+15	100.0	90	0.022
1.0E+15	100.0	30	0.311
1.0E+15	100.0	10	1.024
1.0E+15	100.0	5	0.636
1.0E+16	0.0	90	0.162
1.0E+16	0.0	30	0.183
1.0E+16	0.0	10	0.413
1.0E+16	0.0	5	0.449
1.0E+16	10.0	90	0.163
1.0E+16	10.0	30	0.212
1.0E+16	10.0	10	0.514
1.0E+16	10.0	5	0.513
1.0E+16	100.0	90	0.160
1.0E+16	100.0	30	0.478
1.0E+16	100.0	10	1.402
1.0E+16	100.0	5	1.045
1.5E+17	0.0	90	2.437
1.5E+17	0.0	30	2.748
1.5E+17	0.0	10	6.191
1.5E+17	0.0	5	6.738
1.5E+17	10.0	90	2.437
1.5E+17	10.0	30	2.779
1.5E+17	10.0	10	6.303
1.5E+17	10.0	5	6.810
1.5E+17	100.0	90	2.444
1.5E+17	100.0	30	3.069
1.5E+17	100.0	10	7.288
1.5E+17	100.0	5	7.404

* TEC-Total Electron Content.

Table D-4, Simulation Results for 300 Km Altitude and 100 Km Thickness

TEC*	OFFSET in Km	ELEVATION in Degrees	RANGE ERROR in Km
1.0E+15	0.0	90	0.016
1.0E+15	0.0	30	0.018
1.0E+15	0.0	10	0.045
1.0E+15	0.0	5	0.050
1.0E+15	10.0	90	0.016
1.0E+15	10.0	30	0.047
1.0E+15	10.0	10	0.146
1.0E+15	10.0	5	0.113
1.0E+15	100.0	90	0.022
1.0E+15	100.0	30	0.312
1.0E+15	100.0	10	1.028
1.0E+15	100.0	5	0.640
1.0E+16	0.0	90	0.163
1.0E+16	0.0	30	0.185
1.0E+16	0.0	10	0.454
1.0E+16	0.0	5	0.496
1.0E+16	10.0	90	0.163
1.0E+16	10.0	30	0.213
1.0E+16	10.0	10	0.555
1.0E+16	10.0	5	0.560
1.0E+16	100.0	90	0.168
1.0E+16	100.0	30	0.479
1.0E+16	100.0	10	1.445
1.0E+16	100.0	5	1.091
1.5E+17	0.0	90	2.438
1.5E+17	0.0	30	2.769
1.5E+17	0.0	10	6.817
1.5E+17	0.0	5	7.436
1.5E+17	10.0	90	2.438
1.5E+17	10.0	30	2.800
1.5E+17	10.0	10	6.931
1.5E+17	10.0	5	7.508
1.5E+17	100.0	90	2.444
1.5E+17	100.0	30	3.092
1.5E+17	100.0	10	7.933
1.5E+17	100.0	5	8.107

* TEC-Total Electron Content.

Table D-5, Simulation Results for 300 Km Altitude and 300 Km Thickness

TEC*	OFFSET in Km	ELEVATION in Degrees	RANGE ERROR in Km
1.0E+15	0.0	90	0.016
1.0E+15	0.0	30	0.018
1.0E+15	0.0	10	0.042
1.0E+15	0.0	5	0.045
1.0E+15	10.0	90	0.016
1.0E+15	10.0	30	0.047
1.0E+15	10.0	10	0.142
1.0E+15	10.0	5	0.109
1.0E+15	100.0	90	0.022
1.0E+15	100.0	30	0.311
1.0E+15	100.0	10	1.024
1.0E+15	100.0	5	0.636
1.0E+16	0.0	90	0.162
1.0E+16	0.0	30	0.184
1.0E+16	0.0	10	0.418
1.0E+16	0.0	5	0.449
1.0E+16	10.0	90	0.163
1.0E+16	10.0	30	0.213
1.0E+16	10.0	10	0.519
1.0E+16	10.0	5	0.513
1.0E+16	100.0	90	0.168
1.0E+16	100.0	30	0.479
1.0E+16	100.0	10	1.407
1.0E+16	100.0	5	1.044
1.5E+17	0.0	90	2.438
1.5E+17	0.0	30	2.757
1.5E+17	0.0	10	6.274
1.5E+17	0.0	5	6.741
1.5E+17	10.0	90	2.438
1.5E+17	10.0	30	2.788
1.5E+17	10.0	10	6.384
1.5E+17	10.0	5	6.811
1.5E+17	100.0	90	2.444
1.5E+17	100.0	30	3.080
1.5E+17	100.0	10	7.358
1.5E+17	100.0	5	7.391

* TEC-Total Electron Content.

Table D-6, Simulation Results for 300 Km Altitude and 900 Km Thickness

TEC*	OFFSET in Km	ELEVATION in Degrees	RANGE ERROR in Km
1.0E+15	0.0	90	0.016
1.0E+15	0.0	30	0.018
1.0E+15	0.0	10	0.036
1.0E+15	0.0	5	0.037
1.0E+15	10.0	90	0.016
1.0E+15	10.0	30	0.047
1.0E+15	10.0	10	0.136
1.0E+15	10.0	5	0.101
1.0E+15	100.0	90	0.022
1.0E+15	100.0	30	0.311
1.0E+15	100.0	10	1.018
1.0E+15	100.0	5	0.628
1.0E+16	0.0	90	0.162
1.0E+16	0.0	30	0.182
1.0E+16	0.0	10	0.356
1.0E+16	0.0	5	0.375
1.0E+16	10.0	90	0.163
1.0E+16	10.0	30	0.211
1.0E+16	10.0	10	0.457
1.0E+16	10.0	5	0.438
1.0E+16	100.0	90	0.168
1.0E+16	100.0	30	0.476
1.0E+16	100.0	10	1.342
1.0E+16	100.0	5	0.967
1.5E+17	0.0	90	2.437
1.5E+17	0.0	30	2.727
1.5E+17	0.0	10	5.340
1.5E+17	0.0	5	5.618
1.5E+17	10.0	90	2.437
1.5E+17	10.0	30	2.758
1.5E+17	10.0	10	5.447
1.5E+17	10.0	5	5.686
1.5E+17	100.0	90	2.444
1.5E+17	100.0	30	3.046
1.5E+17	100.0	10	6.384
1.5E+17	100.0	5	6.243

*TEC-Total Electron Content.

Table D-7, Simulation Results for 900 Km Altitude and 100 Km Thickness

TEC*	OFFSET in Km	ELEVATION in Degrees	RANGE ERROR in Km
1.0E+15	0.0	90	0.016
1.0E+15	0.0	30	0.018
1.0E+15	0.0	10	0.032
1.0E+15	0.0	5	0.033
1.0E+15	10.0	90	0.016
1.0E+15	10.0	30	0.047
1.0E+15	10.0	10	0.132
1.0E+15	10.0	5	0.096
1.0E+15	100.0	90	0.022
1.0E+15	100.0	30	0.311
1.0E+15	100.0	10	1.014
1.0E+15	100.0	5	0.623
1.0E+16	0.0	90	0.162
1.0E+16	0.0	30	0.180
1.0E+16	0.0	10	0.316
1.0E+16	0.0	5	0.326
1.0E+16	10.0	90	0.163
1.0E+16	10.0	30	0.209
1.0E+16	10.0	10	0.416
1.0E+16	10.0	5	0.390
1.0E+16	100.0	90	0.168
1.0E+16	100.0	30	0.475
1.0E+16	100.0	10	1.300
1.0E+16	100.0	5	0.918
1.5E+17	0.0	90	2.437
1.5E+17	0.0	30	2.707
1.5E+17	0.0	10	4.733
1.5E+17	0.0	5	4.894
1.5E+17	10.0	90	2.438
1.5E+17	10.0	30	2.738
1.5E+17	10.0	10	4.837
1.5E+17	10.0	5	4.960
1.5E+17	100.0	90	2.444
1.5E+17	100.0	30	3.025
1.5E+17	100.0	10	5.752
1.5E+17	100.0	5	5.503

* TEC-Total Electron Content.

Table D-8, Simulation Results for 900 Km Altitude and 300 Km Thickness

TEC*	OFFSET in Km	ELEVATION in Degrees	RANGE ERROR in Km
1.0E+15	0.0	90	0.016
1.0E+15	0.0	30	0.018
1.0E+15	0.0	10	0.030
1.0E+15	0.0	5	0.031
1.0E+15	10.0	90	0.016
1.0E+15	10.0	30	0.047
1.0E+15	10.0	10	0.131
1.0E+15	10.0	5	0.095
1.0E+15	100.0	90	0.022
1.0E+15	100.0	30	0.311
1.0E+15	100.0	10	1.012
1.0E+15	100.0	5	0.622
1.0E+16	0.0	90	0.162
1.0E+16	0.0	30	0.180
1.0E+16	0.0	10	0.305
1.0E+16	0.0	5	0.314
1.0E+16	10.0	90	0.163
1.0E+16	10.0	30	0.209
1.0E+16	10.0	10	0.405
1.0E+16	10.0	5	0.378
1.0E+16	100.0	90	0.168
1.0E+16	100.0	30	0.474
1.0E+16	100.0	10	1.289
1.0E+16	100.0	5	0.906
1.5E+17	0.0	90	2.437
1.5E+17	0.0	30	2.699
1.5E+17	0.0	10	4.573
1.5E+17	0.0	5	4.714
1.5E+17	10.0	90	2.437
1.5E+17	10.0	30	2.730
1.5E+17	10.0	10	4.677
1.5E+17	10.0	5	4.780
1.5E+17	100.0	90	2.443
1.5E+17	100.0	30	3.015
1.5E+17	100.0	10	5.588
1.5E+17	100.0	5	5.321

* TEC-Total Electron Content.

Table D-9, Simulation Results for 900 Km Altitude and 900 Km Thickness

TEC*	OFFSET in Km	ELEVATION in Degrees	RANGE ERROR in Km
1.0E+15	0.0	90	0.016
1.0E+15	0.0	30	0.018
1.0E+15	0.0	10	0.028
1.0E+15	0.0	5	0.029
1.0E+15	10.0	90	0.016
1.0E+15	10.0	30	0.046
1.0E+15	10.0	10	0.128
1.0E+15	10.0	5	0.092
1.0E+15	100.0	90	0.022
1.0E+15	100.0	30	0.311
1.0E+15	100.0	10	1.010
1.0E+15	100.0	5	0.619
1.0E+16	0.0	90	0.162
1.0E+16	0.0	30	0.178
1.0E+16	0.0	10	0.282
1.0E+16	0.0	5	0.289
1.0E+16	10.0	90	0.163
1.0E+16	10.0	30	0.207
1.0E+16	10.0	10	0.382
1.oE+16	10.0	5	0.352
1.0E+16	100.0	90	0.168
1.0E+16	100.0	30	0.473
1.0E+16	100.0	10	1.265
1.0E+16	100.0	5	0.880
1.5E+17	0.0	90	2.437
1.5E+17	0.0	30	2.677
1.5E+17	0.0	10	4.225
1.5E+17	0.0	5	4.330
1.5E+17	10.0	90	2.437
1.5E+17	10.0	30	2.707
1.5E+17	10.0	10	4.328
1.5E+17	10.0	5	4.395
1.5E+17	100.0	90	2.443
1.5E+17	100.0	30	2.991
1.5E+17	100.0	10	5.232
1.5E+17	100.0	5	4.933

* TEC-Total Electron Content.

APPENDIX E - IONOSPHERE MODEL PROGRAM LISTING

```
      DOUBLE PRECISION U(2),V(2),N(2),RINT(2),RØ(2),RT(2),PI,
     & RSAT(2),DENSITY(3Ø),VPHASE(3Ø),VGROUP(3Ø),ERROR(3Ø),RADIUS(3Ø),
     & EARTHRADIUS,FREQ,TIME,DTOTAL,DELTAR,LATITUDE,DLEG,DISTANCE,DOT,
     & TOP,BOTTOM,THICKNESS,TID,RANGEERROR,OFFSET,DELTAL,
     & ALT(3),THICK(3),TEC(3),OFF(3),LAT(4)
        INTEGER ELEV(4)
      LOGICAL UPDATE,TIDIN
      DATA EARTHRADIUS/6375.DØ/,FREQ/1.575D9/
      DATA PI/3.14159265358979323846264DØ/
        DATA ALT/1ØØ.DØ,3ØØ.DØ,9ØØ.DØ/
        DATA THICK/1ØØ.DØ,3ØØ.DØ,9ØØ.DØ/
        DATA TEC/1.D15,1.D16,1.D17/
        DATA OFF/Ø.DØ,1Ø.DØ,1ØØ.DØ/
        DATA LAT/Ø.DØ,2Ø.829DØ,61.7Ø5DØ,66.486DØ/
        DATA ELEV/9Ø,3Ø,1Ø,5/
        CALL ASSIGN(3,'FILE1',5)
        CALL ASSIGN(4,'GPSRANGE',8)
        DO 33 IALT=1,3
        DO 33 ITHICK=1,3
        DO 33 ITEC=1,3
        DO 33 IOFFSET=1,3
        DO 33 ILAT=1,4

      BOTTOM=ALT(IALT)+EARTHRADIUS+1.D-5
        THICKNESS=THICK(ITHICK)
      TOP=BOTTOM+THICKNESS
      TID=TEC(ITEC)*1.D-9/THICKNESS
      TIDIN=.FALSE.
      OFFSET=OFF(IOFFSET)
      DELTAL=Ø

        REWIND 3
      READ(3,77) NLAYERS
77    FORMAT(I2)
      DO 1Ø LAYER=1,NLAYERS
      READ(3,88) RADIUS(LAYER),DENSITY(LAYER)
88    FORMAT(D2Ø.Ø,D2Ø.Ø)
      RADIUS(LAYER)=RADIUS(LAYER)+EARTHRADIUS
1Ø    CONTINUE



23    CALL VLIGHT(NLAYERS,FREQ,DENSITY,VPHASE,VGROUP,ERROR)
      DO 21 LAYER=1,NLAYERS
21    TYPE *,RADIUS(LAYER),DENSITY(LAYER)
      IF(.NOT.TIDIN) RANGEERROR=Ø
      LATITUDE=LAT(ILAT)*PI/18Ø
      UPDATE=.FALSE.
      RT(1)=EARTHRADIUS*COS(LATITUDE+DELTAL)
      RT(2)=EARTHRADIUS*SIN(LATITUDE+DELTAL)

      RSAT(1)=2ØØØØ
      RSAT(2)=Ø

5     TIME=Ø
      DTOTAL=Ø
      DELTAR=Ø


      RØ(1)=RSAT(1)
      RØ(2)=RSAT(2)
      IF(.NOT.UPDATE) CALL NORMALIZE(RT(1)-RSAT(1),RT(2)-RSAT(2),U)
```

```
      IF(UPDATE) CALL NORMALIZE(2*RT(1)-RINT(1)-RSAT(1),
     & 2*RT(2)-RINT(2)-RSAT(2),U)

      DO 2Ø K=2,NLAYERS
      LAYER=NLAYERS+2-K
      CALL INTERSECT(RØ,U,RADIUS(LAYER),RINT)
      DLEG=DISTANCE(RØ,RINT)
      DTOTAL=DTOTAL+DLEG
      TIME=TIME+DLEG/VGROUP(LAYER)
      DELTAR=DELTAR+ERROR(LAYER)*DLEG
      RØ(1)=RINT(1)
      RØ(2)=RINT(2)
      CALL NORMALIZE(-RØ(1),-RØ(2),N)
      CALL REFRACT(U,N,VPHASE(LAYER),VPHASE(LAYER-1),V)
      CALL NORMALIZE(V(1),V(2),V)
      U(1)=V(1)
      U(2)=V(2)
2Ø    CONTINUE

      CALL INTERSECT(RØ,U,EARTHRADIUS,RINT)
      DLEG=DISTANCE(RØ,RINT)
      DTOTAL=DTOTAL+DLEG
      DELTAR=DELTAR+ERROR(1)*DLEG
      TIME=TIME+
     &      (DISTANCE(RØ,RINT)-DISTANCE(RSAT,RINT)+DISTANCE(RSAT,RT))
     &       /VGROUP(1)
      IF(UPDATE)RANGEERROR=
     & 1ØØØ*(DELTAR+DTOTAL-DISTANCE(RSAT,RINT))-RANGEERROR
      IF(UPDATE.AND.TIDIN) WRITE(4,111)BOTTOM-EARTHRADIUS-1.D-5,
     &THICKNESS,TEC(ITEC),OFFSET,ELEV(ILAT),RANGEERROR
111   FORMAT(2F7.1,1PE8.1,ØPF7.1,I3,F7.3)
      IF(UPDATE) GO TO 99
      UPDATE=.TRUE.
      GO TO 5
99    CONTINUE
      IF(TIDIN)  GO TO 33
      LAYER=NLAYERS

16    IF(RADIUS(LAYER).LT.TOP) GO TO 17
      RADIUS(LAYER+2)=RADIUS(LAYER)
      DENSITY(LAYER+2)=DENSITY(LAYER)
      LAYER=LAYER-1
      GO TO 16

17    RADIUS(LAYER+2)=TOP
      DENSITY(LAYER+2)=DENSITY(LAYER)

18    IF(RADIUS(LAYER).LT.BOTTOM) GO TO 19
      RADIUS(LAYER+1)=RADIUS(LAYER)
      DENSITY(LAYER+1)=DENSITY(LAYER)+TID
      LAYER=LAYER-1
      GO TO 18

19    RADIUS(LAYER+1)=BOTTOM
      DENSITY(LAYER+1)=DENSITY(LAYER)+TID

      NLAYERS=NLAYERS+2
      TIDIN=.TRUE.
      DELTAL=OFFSET/EARTHRADIUS
      GO TO 23
33    CONTINUE
      STOP
      END
```

```
      DOUBLE PRECISION FUNCTION DISTANCE(V1,V2)
C ORDINARY EUCLIDEAN DISTANCE BETWEEN TWO POSITION VECTORS
      DOUBLE PRECISION V1(2),V2(2)
      DISTANCE=SQRT((V1(1)-V2(1))**2+(V1(2)-V2(2))**2)
      RETURN
      END

      DOUBLE PRECISION FUNCTION DOT(V1,V2)
C DOT PRODUCT OF VECTORS
      DOUBLE PRECISION V1(2),V2(2)
      DOT=V1(1)*V2(1)+V1(2)*V2(2)
      RETURN
      END

      SUBROUTINE REFRACT(U,N,C1,C2,V)
C
C [][][][][][][][][][][][][][][][][][][][][][][][][][][][][][][][][][]
C VECTOR REFRACTION SUBROUTINE
C
C U IS THE UNIT INCIDENT VECTOR
C N IS THE UNIT NORMAL ON THE SIDE OPPOSITE THE SIDE OF INCIDENCE
C C1 IS THE PHASE SPEED OF INCIDENCE
C C2 IS THE PHASE SPEED ON OPPOSITE SIDE
C V IS THE UNIT REFRACTED VECTOR
C
C [[[[ IT IS ASSUMED THAT THERE WILL BE REFRACTION INSTEAD OF
C      TOTAL INTERNAL REFLECTION; THE ARGUMENT OF THE SQUARE ROOT
C      WOULD BE NEGATIVE IN THE CASE OF TOTAL INTERNAL REFLECTION ]]]]
C
C [][][][][][][][][][][][][][][][][][][][][][][][][][][][][][][][][][]


      DOUBLE PRECISION U(2),N(2),V(2),C1,C2,FACTOR,UDOTN,DOT
      UDOTN=DOT(U,N)
      FACTOR=SQRT(UDOTN*UDOTN+(C1/C2)**2-1)-UDOTN
      V(1)=C2/C1*(FACTOR*N(1)+U(1))
      V(2)=C2/C1*(FACTOR*N(2)+U(2))
      RETURN
      END

      SUBROUTINE INTERSECT(RØ,U,RS,RINT)
C
C [][][][][][][][][][][][][][][][][][][][][][][][][][][][][][][][][][]
C
C A LINE EXTENDS FROM RØ IN THE DIRECTION INDICATED BY THE UNIT VECTOR U
C A SPHERE OF RADIUS RS IS CENTERED AT THE ORIGIN
C THE LINE FIRST INTERSECTS THE SPHERE AT A DISTANCE P
C THE POINT OF INTERSECTION IS DEFINED BY THE POSITION VECTOR RINT
C RINT=RØ+P*U
C
C [][][][][][][][][][][][][][][][][][][][][][][][][][][][][][][][][][]
C
      DOUBLE PRECISION RØ(2),U(2),RINT(2),P,SQRS,RS,RØDOTRØ,RØDOTU,DOT
      RØDOTRØ=DOT(RØ.RØ)
      RØDOTU=DOT(RØ,U)
      SQRS=RS*RS
      P=(RØDOTRØ-SQRS)/(SQRT(SQRS+RØDOTU*RØDOTU-RØDOTRØ)-RØDOTU)
      RINT(1)=RØ(1)+P*U(1)
      RINT(2)=RØ(2)+P*U(2)
      RETURN
      END

      SUBROUTINE VLIGHT(NLAYERS,FREQ,DENSITY,VPHASE,VGROUP,ERROR)
```

```
C
C [][][][][][][][][][][][][][][][][][][][][][][][][][][][][][][][][][][]
C
C IN THE IONOSPHERE, ELECTRON DENSITY DETERMINES PHASE SPEED AND
C GROUP SPEED OF ELECTROMAGNETIC PHENOMENA OF A SPECIFIED FREQUENCY
C
C IF ONE IGNORES THE DELAY CAUSED BY THE IONOSPHERIC LAYER, A RANGE
C DEVIATION ACCRUES FOR EACH KILOMETER OF THE PATH THROUGH THE LAYER
C
C THE RATIO OF THE RANGE DEVIATION TO THE PATH LENGTH WITHIN THIS
C LAYER IS DEFINED BY THE "VELOCITY DEFECT" C-VG.
C THIS RATIO APPEARS HERE AS THE ARRAY "ERROR".
C
C [][][][][][][][][][][][][][][][][][][][][][][][][][][][][][][][][][][]
C
C
      DOUBLE PRECISION DENSITY(3Ø),VPHASE(3Ø),VGROUP(3Ø),ERROR(3Ø),
     & QE,ME,PI,FREQ,DIFF,C
      DATA QE/4.8Ø298D-1Ø/,ME/9.1Ø91D-28/,PI/3.1415926535898DØ/,
     & C/299792.456DØ/

      DO 1Ø LAYER=1,NLAYERS
      DIFF=DENSITY(LAYER)*QE*QE/(PI*FREQ*FREQ*ME)
      VPHASE(LAYER)=C/SQRT(1-DIFF)
      VGROUP(LAYER)=C*C/VPHASE(LAYER)
      ERROR(LAYER)=
     &(((2.734375D-1*DIFF+3.125D-1)*DIFF+3.75D-1)*DIFF+5.D-1)*DIFF

1Ø    CONTINUE
      RETURN
      END

      SUBROUTINE NORMALIZE(A,B,V)
C A UNIT VECTOR V IS CREATED
C ITS COMPONENTS ARE PROPORTIONAL TO A AND B
C
      DOUBLE PRECISION A,B,V(2),LENGTH
      LENGTH=SQRT(A**2+B**2)
      V(1)=A/LENGTH
      V(2)=B/LENGTH
      RETURN
      END
```

APPENDIX F - COLLISION AVOIDANCE SYSTEMS SURVEY

TABLE F-1. COMPARISON OF PROPOSED AIRBORNE COOPERATIVE COLLISION AVOIDANCE SYSTEM

	BCAS	McDonnell-Douglas CAS	Sierra CAS	MITRE CAS	Litchford CAS	RCA VECAS	Honeywell AVOIDS	GPS with TDMA Data Link
Type of System:	Beacon, active/passive	Time/ Frequency	Time/ Frequency	Beacon	Beacon, active/passive	Beacon	Beacon	GPS Based
Equipped aircraft would receive protection from:	All ATCRBS and DABS equipped	similarly equipped only	similarly equipped only	similarly equipped only	All ATCRBS equipped	similarly equipped only	similarly equipped only	similarly equipped only
Data on intruding planes made available:	relative altitude and velocity	relative altitude and velocity	relative altitude and velocity	relative altitude and velocity	relative altitude and velocity	relative altitude and velocity	relative altitude and velocity	absolute relative position velocity bearing
Subject to garble and interference problems?	Yes	No	No	Yes	Yes	Yes	Yes	No
Reliance on ground facilities:	relies on ground interrogations in terminal areas (passive mode)	relies on ground stations for timing synchronization	relies on modified TACAN/DME equipment for timing	no ground reliance	relies on ground interrogations in terminal area (passive mode)	no ground reliance	no ground reliance	relies only on GPS system (Differential GPS sites could improve accuracy
Unique advantages or disadvantages:	full system is too expensive for GA	timing synchronization is not universally available	timing synchronization is not universally available	saturation problems in dense terminal areas	full system too expensive for GA	excessive false alarms	excessive false alarms	high equipment commonal among CA universal navigative prec. approach landing function

ANTC-117 Specification for a Cooperative Collision Avoidance System

I. Threat Logic

A. Measurements used:

1. range--separation distance between aircraft, computed by pulse timing.
2. range rate--obtained from successive range measurements.
3. barometric altitude--is encoded and communicated.
4. altitude rate--computed from successive altitude measurements.

B. Altitude and rate info is used to reduce threat volume, then Primary Threat Criteria is applied:

$$(\text{Range}) + T \times (\text{range rate}) \leq (\text{min. range})$$

T is a time constant which takes on 2 values:

1. a broad "T_2 criterion" is used first, and if satisfied pilot is commanded to limit turns and neither climb nor dive.
2. then the more restrictive "T_1 criterion" is applied--if satisfied, alarm occurs and vertical escape maneuvers are issed.

C. An alarm will also occur if range is less than a minimum (3040 ft.), regardless of range rate.

II. Time-Frequency technique

A. Each aircraft mutually synchronized to a common time reference; selects exclusive 1.5 ms time slot (2,000 slots/epoch).

B. 4 frequencies used to reduce co-slot interference.

C. Operational avoidance signal transmitted near beginning of time slot; 2 pulses, altitude is encoded in separation; time delay at reception used to compute range.

D. Successive measurements of range, altitude give range rate, altitude rate.

Types of Cooperative Collision Avoidance Systems

Time-frequency (TF): Uses ANTC-117 TF technique. The time division multiplexing reduces interference, "garble." Requires precise time synchronization. Not compatible with ATCRBS or DABS (Discrete Address Beacon System).

ATCRBS: Interrogates existing ATCRBS transponders. Some have passive mode for use in terminal areas, which listens to ground-elicited replies instead of issuing own interrogations. Active mode contributes to garble problems. Both modes very susceptible to interference. Protection from ATCRBS-equipped aircraft realized immediately.

Beacon: Transponder-interrogation techniques like ATCRBS but not compatible with it. Does not add interference to existing ATCRBS system.

DABS: Interrogates DABS transponders and uses air-air and air-ground-air datalink via DABS.

All systems can be implemented with various levels of equipment to provide coverage varying from full CAS protection to inexpensive equipment such as transponder-only systems which do not provide threat evaluation but provide signals which are used in the threat evaluation process by higher-level-equipped craft.

Some Particular Collision Avoidance Systems

Comments on Operation and Performance

TF Systems:

(1) McDonnel Douglas CAS -- Conforms to ANTC-117 guidelines; produces excessive number of alarms.

(2) Sierra CAS (proposed) -- Uses ground TACAN/DME stations for time synchronization, modified TACAN airborne equipment for CAS.

ATCRBS Systems:

(1) MITRE CAS -- Interrogates azimuthal sections using switched directional antennas, multiple power levels. Unsatisfactory in some dense terminal areas.

(2) Litchford CAS -- Has active and passive modes.

(3) BCAS -- Has active and passive mode for detection of ATCRBS and DABS equipped aircraft; air-air and air-ground-air data link via DABS.

Beacon Systems:

(1) RCA SeCANT VECAS -- Interrogates by "addressing" separate altitude layers. Has problems with range rate accuracy; false alarms.

(2) Honeywell AVOIDS -- Very similar to RCA. Has problems with false tracks.

Bagnall, "Collision Avoidance: The State of the Art and Some Recent Developments and Analyses," Navigation, Vol. 23, no. 3, Fall 1976.

I. Specification for cooperative CAS (ANTC-117) ("ATA logic")

A. Committee (ANTC-117) formed 1966, spec published 1967, then revised later.

B. ANTC-117 logic:

(1) based on RF measurements of RANGE & RATE (doppler)
(2) data exchange of altitude

C. Specific technique described:

(1) highly stable, synchronized oscillators for one-way range and rate measurements.
(2) synchronized time multiplex arrangement that eliminates mutual interference -- "time-frequency" technique.

D. Primary Threat Criteria:

$$R + T_i\dot{R} \leq Ro_i \qquad \text{or} \qquad R \leq Rm$$

(1) T_1 = 25 sec., Ro_1 = 1/4 n.m. (1520 ft.) Rm = 1/2 n.m. (3040 ft.)
(2) T_2 = 40 sec., Ro_2 = 1.8 n.m. (10,960 ft)

E. Vertical Escape maneuvers only.

II. Time-frequency (TF) Techniques

A. Makeup of transmitted signal

B. Time synchronization method.

III. Sierra CAS (Proposed)

A. Uses ground TACAN/DME stations for synchronization and modified TACAN airborne equip. for CAS.

B. Range differencing for rate estimation.

(1) excessive error
(2) more sensitive to multipath than TF

IV. Beacon Techniques

A. RCA SECANT (SEparation and Control of Aircraft using Nonsynchronous Techniques) VECAS (Vertical Escape CAS) (full & GA)

(1) interrogation waveform: 2-pulse, delay proportional to barometric altitude - (one-pulse replies)
(2) series of altitude bands (500 ft. wide) is "addressed" by varying the delay -- only transponders in the selected altitude band will respond.
(3) frequency multiplexing & correlation also used to reduce "Fruit effects" (interference).
(4) VECAS cycles thru 3 steps: (for each altitude layer)
    (a) search for targets (uses "range bins")
    (b) tracking & fine range measurement; uses differencing for range rate
    (c) altitude decoding & threat estimation

B. Honeywell AVOIDS I & II - similar to RCA except:

(1) no fine altitude by communication -- overlapping altitude layers are addressed to logically determine altitude of replying transponder relative to ATA criteria boundaries.
(2) has "ghosting" problems

V. Other Approaches to CAS--use existing ATCRBS transponders

A. Mitre CAS

(1) minimize interference by limiting number of CAS units
(2) directive antennas & multiple power levels of interrogations reduce garble (& "defruiter")
(3) range measured directly, altitude decoded from reply
(4) FAA tested simple version in Fall 1975 without mult. power levels or directional antennas

B. Litchford CAS

(1) passive (primary) mode

(a) receives SSR (secondary surveillance radar) interrogations and stimulated replies from ATCBRS transponders
(b) measures & stores difference in time-of-arrival (Δ TOA).
(c) decode transponder message for altitude & identity
(d) using stored data from interrogations of 2 or more SSR's, range & bearing computed

(2) active mode

(a) when less than 2 SSR's available
(b) interrogate transponders actively
(c) range rate from differential range

VI. IDA (Institute for Defense Analyses) Analysis

A. Range rate estimation using incremental range can have a computational bias error.

(1) error increases with time between range measurements.
(2) Sierra CAS has poor range rate accuracy
(3) RCA has small bias error due to short time between range measurements

Klass, "Collision Avoidance Standard Prepared," Aviation Week & Space Technology, Sept. 4, 1978

I. FAA Standard to be issued late 1978

A. Active-type, airborne, beacon-based CAS (B-CAS)

B. No mandatory use envisioned

C. System will provide conflict alert and escape maneuver commands for equipped airplane involved in potential threat with another craft having only conventional radar transponder.

D. Aircraft equipped with BCAS will be required to turn them off in high traffic near airports due to excessive interference they would cause.

II. "Full-capability" B-CAS being developed and studied

A. Usable in high-density terminal areas

B. Incorporates the "best" of earlier proposed techniques:

(1) Passive-mode "listen-in" technique proposed by Litchford Electronics.
(2) "Single-site" (SS-CAS) proposed by Schuchman of Stanford Telecom; would install transponder at each interrogator site.
(3) DABS (discrete address beacon system) - compatible B-CAS, by Koenke of FAA.

III. DABS - each aircraft interrogated individually by its "discrete address" code -- 2-way data link

--ground equipment for threat evaluation and evasive maneuver generation

--ATARS= automatic traffic advisory and resolution systems

--possible conflicts between computer's solution to a threat and what human controller might prefer to use

IV. FAA Task Force's recommendations:

A. Fast implementation of automatic conflict alert in the ARTS-3 terminal area systems (Automated Radar Terminal Systems).

B. Rapid implementation of DABS (TI-built prototype is being tested).

C. Increased use of radar transponders.

D. Implementation of ATARS.

E. Establish national standard for an active B-CAS.

BCAS: Beacon Collision Avoidance System
FAA-NAFEC (1977)

I. Passive mode

A. Detects ATCRBS interrogations and replies from other aircraft. Mode C replies provide altitude. Time difference between interrogations and subsequent replies is used to compute parameters. Interrogations and replies from 2 or more ground based systems are required for range and azimuth computation. Threat potential is then evaluated.

II. Active mode operation

A. Computer-controlled interrogation sequence repeats at 1-sec. intervals:

(1) activate top antenna
(2) xmit pair of mode C pulses
(3) wait for all replies in range (500μS) (=32mi. radius).
(4) xmit pair of suppression pulses from top followed by mode C pulses from bottom antenna

B. Computer program correlates replies from successive interrogations to determine range rate and altitude rate.

(1) track is established for each aircraft replying coherently to four successive interrogations.

(2) tracks with negative range rate (closing) are updated each second. Positive rate tracks are discontinued.

(3) track is "coasted" during missed replies (after 8 missed, track is discontinued).

C. Special interrogation sent to each new track to determine if BCAS-equipped. If so, complementary maneuvers will be coordinated in event of threat via BCAS air-air data link.

D. In event of threat, climb or dive maneuvers are issued to pilot. (ANTC 117 threat logic used).

III. Systems Enhancements

A. "Whisper/Shout" -- multi-level power xmission of interrogations to break up responding population into smaller groups. (Phase II)

B. Phase III -- compatibility with DABS (Discrete Address Beacon System) DABS will be used for air-air data link and air-ground-air data link.

C. Passive, Semi-active, and Active modes to be implemented automatically.

MCDONNEL DOUGLAS COLLISION AVOIDANCE SYSTEM

Operational Concept

The MDEC CAS is an air-derived CAS employing time/frequency multiplexing. Timing synchronization is provided by ground stations and through air-to-air relay by appropriately equipped aircraft. Each synchronized CAS transmits in an exclusive time/frequency slot and receives the transmissions of other CASs in their respective slots. The information exchanged in this fashion includes one-way range and altitude. Range rate is computed from successive measurements of range. The information is used by the CAS to evaluate the threat of collision based on ANTC-117 logic.

Two levels of CAS equipment are available: a full system intended primarily for air carrier use, and a limited system for general aviation. The latter system has a shorter range and cannot participate in air-to-air relay of synchronization signals.

The MDEC CAS has a Back-Up Mode (BUM) which is used when no timing synchronization is available. In BUM, asynchronous interrogation-reply techniques are used. To reduce interference in BUM, a CAS will respond to an interrogation only if the interrogator is within 3300 ft. of own altitude and has a closing range rate of greater than 117 knots. Barometric altitude is encoded in the interrogation, and relative range rate is determined from the spacing of two successive interrogations. The response is one of four messsages encoded in the spacing between pulses determined by the altitude difference: aircraft above, aircraft below, dive, or climb. The chance of overlapping interrogations is reduced by choosing a 6 ms signal-free interval out of the 3-second cycle time in which to interrogate.

In the normal (synchronized) mode, the 3-second cycle or epoch is divided into 2,000 1.5 ms time slots. Four different frequencies are used (1600, 1605, 1610, 1615 MHz) to minimize co-slot interference. A range pulse is transmitted near the start of the time slot, followed by an altitude pulse delayed by an amount proportional to the barometric altitude of the aircraft. Other synchronized CAS's can compute their range from the propagation time of the range pulse and decode the altitude information.

Performance

The computation of range rate by using successive range measurements is biased and will not always give an accurate estimate of relative velocity (range rate). The MDEC CAS uses the difference between current range and the range at six seconds previous to estimate current range rate. The bias error resulting is a function of the range and the actual range rate, and results in an overestimate of range rate. The net result is premature and false alarms - typically an estimated 8 to 10 percent increase in overall alarm rate.

Otherwise, the MDEC CAS performed well by ANTC-117 guidelines. The nominal communication range is 126 nmi, but can fluctuate considerably due to the nulls and fades of the airborne antenna gain pattern such that there is a 10 percent probability that the range is less than 47 nmi. Timing standards for the full CAS are accurate to one part in 10^8. Under the best of circumstances, this will result in synchronized status being lost in 4.25 minutes if no synchronization updates are obtained.

Interference in Back-Up Mode (BUM) can cause missed alarms or incorrect decoding of the warning signal. Since BUM is only entered during lack of synchronization, however, it will usually be used in low-density areas.

RCA COLLISION AVOIDANCE SYSTEM

Operational Concept

The RCA SECANT (Separation Control of Aircraft using Nonsynchronous Techniques) equipment comes in three levels: VECAS (Vertical Escape CAS), for large commercial transport aircraft; VECAS-GA for smaller general aviation aircraft; and PWI (Proximity Warning Indicator), for aircraft that cannot afford a complete CAS. The SECANT equipment is of the beacon/transponder type. Several techniques are employed to reduce the incidence of self-generated interference or "fruit" which is a problem when this type of system is used in high-density areas:

1. Frequency multiplexing: Twenty-four frequency assignments are used; 12 above 10,000 ft. and 12 below. Of these 12, six are used with the top antenna and 6 with the bottom. Of the six, two are used for probes (interrogations) and four for replies. For each probe frequency, there is a corresponding pair of reply frequencies. These two frequencies are used for binary encoding of altitude on the reply.
2. Pseudo noise correlation of replies: The interrogator transmits a sequence of probes, randomly selecting which of the appropriate pair of probe frequencies will be used for a given probe. Replies to this interrogation sequence will be correlated with the randomly selected pattern on the associated reply frequencies; whereas, unwanted fruit replies will not. This is used to reject fruit.
3. Asynchronous interrogations: Probe transmissions are jittered randomly in time with an average period of 1 msec. This reduces fruit, since the fruit tends to be uniformly distributed in time relative to any asynchronous probe and will therefore not be mistaken for a true target.

4. Altitude layer addressing: Interrogations consist of two pulses time delay coded to "address" different altitude layers. Layers are 500 ft. wide below 10,000 ft. and 1,000 ft. above. Only transponders in the addressed layer will reply to a given interrogation. The number of altitude layers interrogated above and below the aircraft is dependent on its altitude and the direction and magnitude of its vertical velocity, so that only layers which might contain threats are interrogated.

The VECAS equipment has three modes of operation: (1) target searching, (2) tracking during which fine target range is measured and range rate is estimated (using range differencing), and (3) data communications during which altitude and identity are decoded from the replies.

Performance

Round time, the period required to evaluate all targets, for the VECAS varies from less than 3 sec. to 4.26 sec. maximum. Range and range rate accuracies are compatible with ANTC-117. In high density areas, the resulting increased fruit rate can cause false targets, missed targets, and incorrect range measurements. Another problem results from multiple targets occupying the same "range bin," in which case only one of them will be tracked and its accuracy will be corrupted. Bin straddling can also result, causing one target to appear as 2 or 3 separate targets, thus increasing the effective round time. The data transfer technique appears to be highly reliable, with an estimated 99 percent probability of correctly receiving a message in one try.

Honeywell Collision Avoidance System

Operational Concept

The Honeywell CAS is a beacon-transponder type of system, utilizing asynchronous transponder ranging. The interrogation and reply waveforms are transmitted on the same frequency (1600 MHz). A reference altitude is coded in the delay between pulses of the interrogation waveform, which is used to "address" distinct altitude bands. An aircraft's transponder will reply to an interrogation only if its altitude is within 700 ft. of the reference altitude. Fine altitude measurements are logically determined from the results of addressing several altitude bands which overlap.

Range is determined from the time delay of the replies. Range rate is determined from successive range measurements. Collision threat is evaluated using ANTC-117 logic. Replies received within the maximum range limit are detected and assigned to range bins. Epoch length, or round time, is 3 seconds. Within each epoch a maximum of seven sets of range data are obtained. These data sets are used to determine if a threatening track exists. The range tracking filter utilizes a technique called inhibit/suppression logic to eliminate false tracks generated by interactions of real tracks.

Performance

The Honeywell CAS has adequate communication range for threat evaluation. Alarms generated by false tracks are considered excessive. The rate of false alarms in dense terminal area traffic was estimated at one in five hours for the pilot, but about 200 per hour for the ground controllers. These false tracks are generated by fruit and combinations of other tracks, the latter being the more significant source. The inhibit/suppression logic which can reduce these levels can also cause genuine threatening targets to be ignored. Changes have been suggested which can reduce false tracks without the inhibit/suppression logic. Transponder blockage from real and fruit-generated interrogations can be serious, but changes have been suggested which can reduce its occurrence to an acceptable rate of 3 percent.

Sierra DME Collision Avoidance System

Operational Concept

The CAS proposed by Sierra, designated DME/CAS (Distance Measuring Equipment CAS), is an air-derived synchronous concept intended to exploit the proliferation of DME ground facilities to obtain timing synchronization, and to adapt DME airborne equipment to fulfill the CAS function. DME ground facilities would be augmented to transmit a CAS time reference signal (CASTRS), in addition to normal DME replies. Airborne clocks, included in the DME/CAS units, would be synchronized to the received reference after correction for the propogation delay obtained by DME techniques.

Overall system operation is as follows. The airborne CAS synchronizes its clock to the DME ground station's reference signal. The synchronization signal provides the common timing format for a time-division multiplexing scheme in which a 3-second epoch is divided into 2000 1.5ms time slots. After synchronization, the airborne CAS selects an unoccupied time slot for transmission of the CAS signal, from which other synchronized CAS units can decode one-way range information. Barometric altitude is encoded using pulse-delay encoding into the CAS signal. Range rate is obtained from the difference in range in successive epochs. These three measurements are used in accordance with ANTC-117 logic to determine collision threat potential.

The DME/CAS frequencies are selected from the 960 to 1213 MHz band allocated to DME service.

Performance

Some potential problems with the DME/CAS concept are interslot interference, overloading of DME ground transponders, threat parameter measurement inaccuracies, and undetected co-slot occupancy.

Using two frequencies for the CAS function should provide adequate protection against interslot interference, such that adjacent time slots use different frequencies. DME ground transponder capacity would be reduced by only 3 percent if the transmission of the CASTRS is given priority over DME replies. Threat parameter measurement accuracies can meet the specifications of ANTC-117 only if the DME ground facility standards on accuracy are upgraded. The effect of the bias error introduced into the range rate

measurement by using the range differencing technique should be only an 8 to 10 percent increase in overall alarm rate. The probability of undetected co-slot occupancy has been estimated to be 1 to 4 percent in dense traffic, but these occurrences could be rendered unambiguous by properly designed pulse decoders such that the potential threat can still be detected.

With two frequency channels, and appropriate pulse decoders, the DME/CAS should have more than adequate capacity to accommodate the 297 aircraft of the Los Angeles Basin 1982 model.

CAS Survey References

1. "A Review and Analysis of the Honeywell Collision Avoidance System," Phase I, Vols. I and II, Report No. FAA-RD-73-151 (IDA Study S-424), Oct. 1973.

2. "A Review and Analysis of the McDonnell Douglas Collision Avoidance System," Phase I, Report No. FAA-RD-73-143 (IDA Study S-425), Oct. 1973.

3. "A Review and Analysis of the RCA Collision Avoidance System," Phase I, Report No. FAA-RD-73-152 (IDA Study S-426), Oct. 1973.

4. "A Review and Analysis of the Honeywell Collision Avoidance System," Phase II, Report No. FAA-RD-75-151 (IDA Study 5-460), Oct. 1975.

5. "A Review and Analysis of the McDonnell Douglas Collision Avoidance System," Phase II, Report No. FAA-RD-75-143 (IDA Study S-458), Oct. 1975.

6. "A Review and Analysis of the RCA Collision Avoidance System," Phase II, Report No. FAA-RD-75-152 (IDA Study S-462), Oct. 1975.

7. "A Review and Analysis of the Sierra DME Collision Avoidance System," Report No. FAA-RD-75-141 (IDA Study S-456), Oct. 1975.

8. "A Review and Analysis of Some Collision Avoidance Algorithms with Particular Reference to ANTC-117," Report No. FAA-RD-75-72 (IDA Study S-450), June 1975.

9. Bagnall, J. J., "Collision Avoidance: The State of the Art and Some Recent Developments and Analyses," Navigation, Vol. 23, No. 3, Fall 1976.

10. Richardson, C. A., and Cohen, M., "A Computer Controlled Aircraft Collision Avoidance System," American Institute of Aeronautics and Astronautics, 1977.

11. Orlando, V. A., and Welch, J. D., "Beacon CAS (BCAS), An Integrated Air/Ground Collision Avoidance System," Report No. FAA-RD-76-2, March 23, 1976.

12. Hwoschinsky, P. V., and Koenke, E. J., "A Single Site Passive Collision Avoidance System," 33rd annual meeting of the Institute of Navigation, June 1977.

13. Klass, P. J., "Collision Avoidance Plan Views Diverge," Aviation Week & Space Technology, July 23, 1979.

1. Report No.	2. Government Accession No.	3. Recipient's Catalog No.
NASA CR-165675		

4. Title and Subtitle	5. Report Date
Feasibility of Collision Warning, Preceision Approach and Landing Using the GPS	March 1981
	6. Performing Organization Code
7. Author(s)	8. Performing Organization Report No.
W. H. Ruedger	RTI/1825/01-01F
	10. Work Unit No.
9. Performing Organization Name and Address	11. Contract or Grant No.
Research Triangle Institute Post Office Box 12194 Research Triangle Park, NC 27709	NAS1-15833
	13. Type of Report and Period Covered
12. Sponsoring Agency Name and Address	Contractor Report May 1979 to July 1980
National Aeronautics and Space Administration Langley Research Center Hampton, VA 23665	14. Sponsoring Agency Code

15. Supplementary Notes

Langley Contract Monitor - W. E. Howell

Final Report

16. Abstract

This report presents conceptual approaches wherein GPS may be used, with an appropriately configured data link, to enhance general aviation avionic functions encountered in the terminal area and on approach. Functions specific to this study are approach and landing guidance and collision warning.

One effort of this study explored the feasibility of using differential GPS to obtain the precision navigation solutions required for landing. The study established that the concept is sound and developed an experimental program with the objective of demonstrating this concept. Other effort, of comparable emphasis, generated the foundation and guidelines involved in the use of GPS, with an associated data link, to provide collision avoidance and/or warning. This effort examined the collision avoidance/warning concept through the development of a functional system specification.

17. Key Words (Suggested by Author(s))	18. Distribution Statement
Differential GPS Ionosphere Variability Data Link TDMA	

19. Security Classif. (of this report)	20. Security Classif. (of this page)	21. No. of Pages	22. Price*
Unclassified	Unclassified	119	

N-305

End of Document